

Dinoflagellate cyst assemblages as tracers of sea-surface conditions in the northern North Atlantic, Arctic and sub-Arctic seas: the new 'n = 677' data base and its application for quantitative palaeoceanographic reconstruction

ANNE DE VERNAL,^{1*} MARYSE HENRY,¹ JENS MATTHIessen,² PETA J. MUDIE,³ ANDRÉ ROCHON,³
KARIN P. BOESSENKOOL,⁴ FRÉDÉRIQUE EYNAUD,⁵ KARI GRØSFJELD,⁶ JOËL GUIOT,⁷ DOMINIQUE HAMEL,¹
REX HARLAND,⁸ MARTIN J. HEAD,⁹ MARTINA KUNZ-PIRRUNG,² ELISABETH LEVAC,¹⁰ VIRGINIE LOUCHEUR,¹
ODILE PEYRON,¹ VERA POSPELOVA,¹¹ TAOUFIK RADI,¹ JEAN-LOUIS TURON⁵ AND ELENA VORONINA,¹

¹ GEOTOP, Université du Québec à Montréal, P.O. Box 8888, Montréal, Québec, H3C 3P8, Canada

² Alfred Wegener Institute for Polar and Marine Research, P.O. Box 120161, D27515, Bremerhaven, Germany

³ Geological Survey of Canada, Atlantic, Box 1006, Dartmouth, Nova Scotia, B2Y 4A2, Canada

⁴ Laboratory of Palaeobotany and Palynology, Utrecht University, Budapestlaan 4, 3584 CD Utrecht, The Netherlands

⁵ Département de Géologie et Océanographie, UMR 5805 CNRS, Université Bordeaux I, avenue des facultés, 33405 TALENCE Cedex, France

⁶ Geological Survey of Norway, PO Box 3006, Lade, N-7002, Trondheim, Norway

⁷ CNRS-CEREGE, B.P. 80, 13545 Aix en Provence, Cedex 4, France

⁸ DinoData Services, 50 Long Acre, Bingham, NG13 8AH, England and Centre for Palynology, University of Sheffield, Dainton Building, Brook Hill, Sheffield, S3 7HF, England

⁹ Department of Geography, University of Cambridge, Downing Place, Cambridge CB2 3EN, England

¹⁰ Department of Earth Sciences, Dalhousie University, Halifax, Nova Scotia, B3H 3J5, Canada

¹¹ Department of Geography and Center for Climate and Global Change Research, McGill University, 805 Sherbrooke Street West, Montréal, Québec, H3A 2K6, Canada

de Vernal, A., Henry, M., Matthiessen, J., Mudie P. J., Rochon A., Boessenkool K. P., Eynaud F., Grøsfjeld K., Guiot J., Hamel, D., Harland, R. Head, M. J., Kunz-Pirring, M., Levac, E., Loucheur, V., Peyron, O., Pospelova, V., Radi, T., Turon, J.-L. and Voronina, E. 2001. Dinoflagellate cyst assemblages as tracers of sea-surface conditions in the northern North Atlantic, Arctic and sub-Arctic seas: the new 'n = 677' data base and its application for quantitative palaeoceanographic reconstruction. *J. Quaternary Sci.*, Vol. 16 pp. 681–698. ISSN 0267-8179.

ABSTRACT: The distribution of dinoflagellate cyst (dinocyst) assemblages in surface sediment samples from 677 sites of the northern North Atlantic, Arctic and sub-Arctic seas is discussed with emphasis on the relationships with sea-surface parameters, including sea-ice cover, salinity and temperature of the coldest and warmest months. Difficulties in developing a circum-Arctic data base include the morphological variation within taxa (e.g. *Operculodinium centrocarpum*, *Islandinium? cezare* and *Polykrikos* sp.), which probably relate to phenotypic adaptations to cold and/or low salinity environments. Sparse hydrographical data, together with large interannual variations of temperature and salinity in surface waters of Arctic seas constitute additional limitations. Nevertheless, the use of the best-analogue technique with this new dinocyst data base including 677 samples permits quantitative reconstruction of sea-surface conditions at the scale of the northern North Atlantic and the Arctic domain. The error of prediction calculated from modern assemblages is ± 1.3 °C and ± 1.8 °C for the temperature of February and August, respectively, ± 1.8 for the salinity, and ± 1.5 months yr⁻¹ for the sea-ice cover. Application to late Quaternary sequences from the western and eastern subpolar North Atlantic (Labrador Sea and Barents Sea) provide reconstructions compatible with those obtained using the previous dinocyst data base ($n = 371$), which mainly included modern data from the northern North Atlantic. Copyright © 2001 John Wiley & Sons, Ltd.

KEYWORDS: dinoflagellate cysts; northern North Atlantic and Arctic; temperature; salinity; sea-ice.

* Correspondence to: A. de Vernal, GEOTOP, Université du Québec à Montréal, P.O. Box 8888, Montréal, Québec, H3C 3P8, Canada. E-mail: r21024@er.uqam.ca

Contract/grant sponsor: Natural Science and Engineering Research Council (NSERC) of Canada.

Contract/grant sponsor: Fonds pour la Formation de Chercheurs et l'aide à la Recherche (FCAR) of Quebec.

Contract/grant sponsor: CNRS (France).

Contract/grant sponsor: Programme National d'Etude du Climat (PNEDC).

Contract/grant sponsor: European Community.

JQS

Journal of Quaternary Science

Introduction

Organic-walled dinoflagellate cysts, or dinocysts, are useful proxies for the reconstruction of past sea-surface conditions, particularly in high-latitude marine environments. In contrast to siliceous or carbonate microfossils, dinocysts are generally well preserved in sediments affected by dissolution because they are composed of highly resistant refractory organic matter. Some dinocysts can be affected by oxidation of their organic wall under specific circumstances, in pelagic sediments with low accumulation rates (e.g. Zonneveld *et al.*, 2001), but preservation in shelf and slope sediments is usually excellent (e.g. McCarthy *et al.*, 2000). Moreover, dinoflagellate populations may thrive despite extremely cold conditions, and relatively abundant dinocysts can be found in sediments of most circumpolar environments of both hemispheres (e.g. Mudie, 1992; Harland and Pudsey, 1999). The encystment and dormancy period, which characterises the life cycle of many dinoflagellates in relation to their sexual reproduction, undoubtedly constitutes an adaptive strategy to disperse and survive in environments marked by seasonally adverse conditions (e.g. Dale, 1983, 1996). The encystment strategy together with heterotrophism of some taxa probably explains how dinoflagellates are able to occupy polar seas where extensive sea-ice cover prevails for a large part of the year and restricts vegetative activity based on autotrophy. Thus, dinoflagellates occupy a wide range of marine environments with respect to temperature, sea-ice cover and salinity, and diversified dinocyst assemblages accordingly can be recovered from high-latitude marine basins and epicontinental seas.

Previous studies of dinocysts in surface sediments from the northern North Atlantic and adjacent basins demonstrated close relationships between the distribution of assemblages and sea-surface conditions, notably temperature, salinity and seasonal duration of sea-ice cover (e.g. Harland, 1983; Turon, 1984; Mudie and Short 1985; Rochon and de Vernal, 1994; Matthiessen, 1995; Kunz-Pirrung, 1998). On these grounds, dinocyst data were used for quantitative reconstruction based on the modern analogue technique (de Vernal *et al.*, 1993a, 1994, 1997; Rochon *et al.*, 1999). They permitted quantitative estimates of late Quaternary sea-surface temperature, salinity and sea-ice cover along the continental margins of eastern Canada (de Vernal *et al.*, 1993b, 1996; Levac and de Vernal, 1997; Levac *et al.*, 2001) and western Europe (Rochon *et al.*, 1998; Eynaud, 1999; Grøsfjeld *et al.*, 1999). They also were used to reconstruct sea-surface conditions throughout the northern North Atlantic during the Last Glacial Maximum (de Vernal *et al.*, 2000). The palaeoceanographic records available from dinocyst data are particularly interesting from an ocean dynamics viewpoint because they permit the reconstruction of sea-ice cover that regulates the albedo and energy exchange at the water–atmosphere interface (de Vernal and Hillaire-Marcel, 2000). These records also enable evaluation of the potential density of surface waters, calculated from temperature and salinity estimates, which may help to constrain variation in the vertical structure of water masses when combined with data from isotopic measurements in planktonic and benthic foraminifers (e.g. Hillaire-Marcel *et al.*, 2001a,b).

In order to enlarge the domain of the dinocyst-based reconstructions for the study of the ocean dynamics in circum-Arctic regions, we have collectively undertaken the enlargement of the northern North Atlantic dinocyst data base to a multibasin scale with the addition of modern samples from the Arctic and sub-Arctic seas, and subpolar North Pacific. Workshops held in 1999 and 2000 helped the development

of a standardised taxonomy, which was indispensable prior to combining data sets established on regional scales in different laboratories and to build the circum-polar data base. Here, we present the updated dinocyst data base that includes the previously published 371 assemblage counts from the northern North Atlantic (de Vernal *et al.*, 1997; Rochon *et al.*, 1999), to which are now added data from the Laptev Sea (Kunz-Pirrung, 1998, this issue), the Bering and Chukchi seas (Radi *et al.*, this issue), the Irminger Sea (Boessenkool *et al.*, this issue), the Barents Sea (Voronina *et al.*, this issue), the Canadian Arctic (Hamel, 2001; Mudie and Rochon, this issue), the Norwegian coasts (Grøsfjeld and Harland, this issue), and many sites from the northern North Atlantic and Kara Sea (Plate 1 and Fig. 1). The new data base comprises a total of 677 reference sites. In the present paper, we report on the particularities of this data base with respect to taxonomy and hydrographic conditions. We report on the procedure developed using the best-analogue method for the reconstruction of past sea-surface salinity, temperature and sea-ice cover and, finally, we discuss the uses and limitations of such an approach with reference to examples of late Quaternary reconstructions. One example is from the Labrador Sea in the northwest North Atlantic, and the other from the Barents Sea in an area close to the boundary between Arctic waters and the northeastern end-member of the North Atlantic drift.

The new circum-Arctic data base

The dinocyst data

The standardisation of laboratory procedures and taxonomy is a prerequisite to the development of joined data bases. The protocol for preparation used for all samples of the data base can be found in de Vernal *et al.* (1999) or Rochon *et al.* (1999), for example. It consists simply of HCl and HF treatments of the greater than 10 µm or 7 µm fraction, and avoids oxidising treatment that may affect the preservation of organic-walled cysts (e.g. Marret, 1993). The dinocyst nomenclature conforms to Head (1996a), Rochon *et al.* (1999) and Head *et al.* (this issue). Three taxa that were not included in the northern North Atlantic data base (de Vernal *et al.*, 1997; Rochon *et al.*, 1999) have been added to the $n = 677$ data base (Table 1). They include cysts of *Polykrikos kofoidii*, which occurs in the Bering Sea (Radi *et al.*, this issue), and cysts belonging to the genus *Polykrikos* referred to as cyst of *Polykrikos* sp. Arctic morphotype. This morphotype shows a wide range of variation, but is distinguished by its smaller size and reduced ornamentation in comparison to the cysts of *Polykrikos schwartzii*. It has been described informally by Kunz-Pirrung (1998) and Radi *et al.* (this issue), and seems to be a characteristic taxon of Arctic environments (Fig. 2). Other new taxa used for statistical treatment in the $n = 677$ data base include *Quinquecuspis concreta*, which has been treated separately from other protoperidinioids, as it constitutes a characteristic taxon of the North Pacific and Bering Sea.

Various morphotypes of *Operculodinium centrocarpum* (de Vernal *et al.*, 1989; Radi *et al.*, this issue) also have been distinguished in the data base because of significant variations in the ornamentation of the cyst wall, and in the density, length and shape of the processes. These morphotypes include the form with short processes (e.g. Rochon *et al.*, 1999), and the morphotype *cezare* first described by de Vernal *et al.* (1989) from post-glacial Champlain Sea sediments of Quebec. The latter constitutes the end member of a gradational lineage

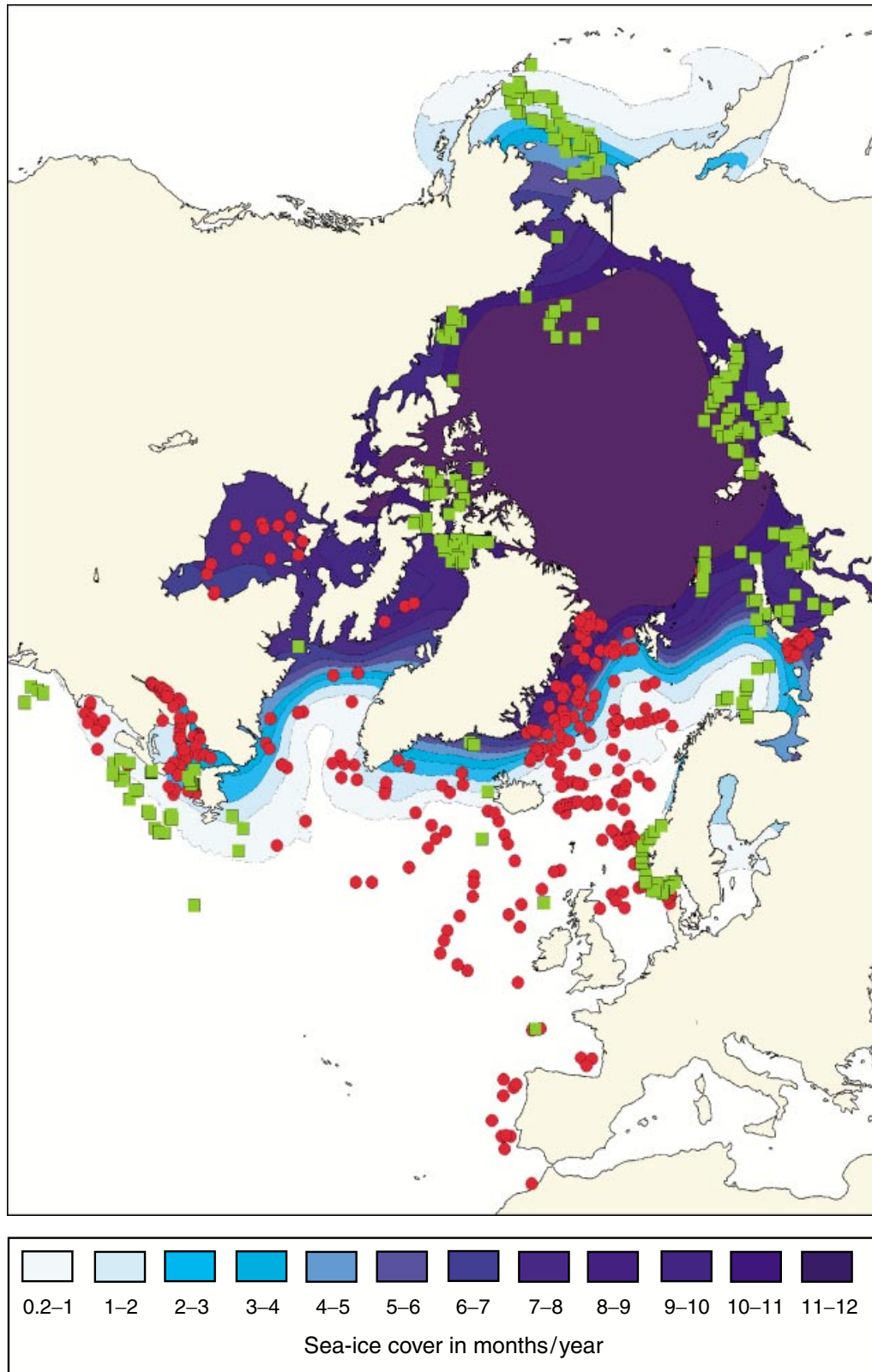


Plate 1 Location map of surface sediment samples used to establish the reference dinocyst data base. The circles correspond to references sites of the 'n = 371' data base as published by de Vernal *et al.* (1997) and Rochon *et al.* (1999). The squares correspond to the additional reference sites included in the 'n = 677' data base. The modern sea-ice cover (in months yr⁻¹ with >50% of sea-ice concentration) is illustrated after data sets provided by the National Climate Data Center (NCDC) in Boulder, Colorado, which span the years 1953 to 1990. Note that the NCDC data set is incomplete for some epicontinental areas such as the Okhotsk Sea (no data reported) and the Gulf of St Lawrence (data extrapolated after Markham, 1980). Note also that interpolation for mapping was done using a window of 3°, which results in smoothing of the very sharp sea-ice gradients along the polar front

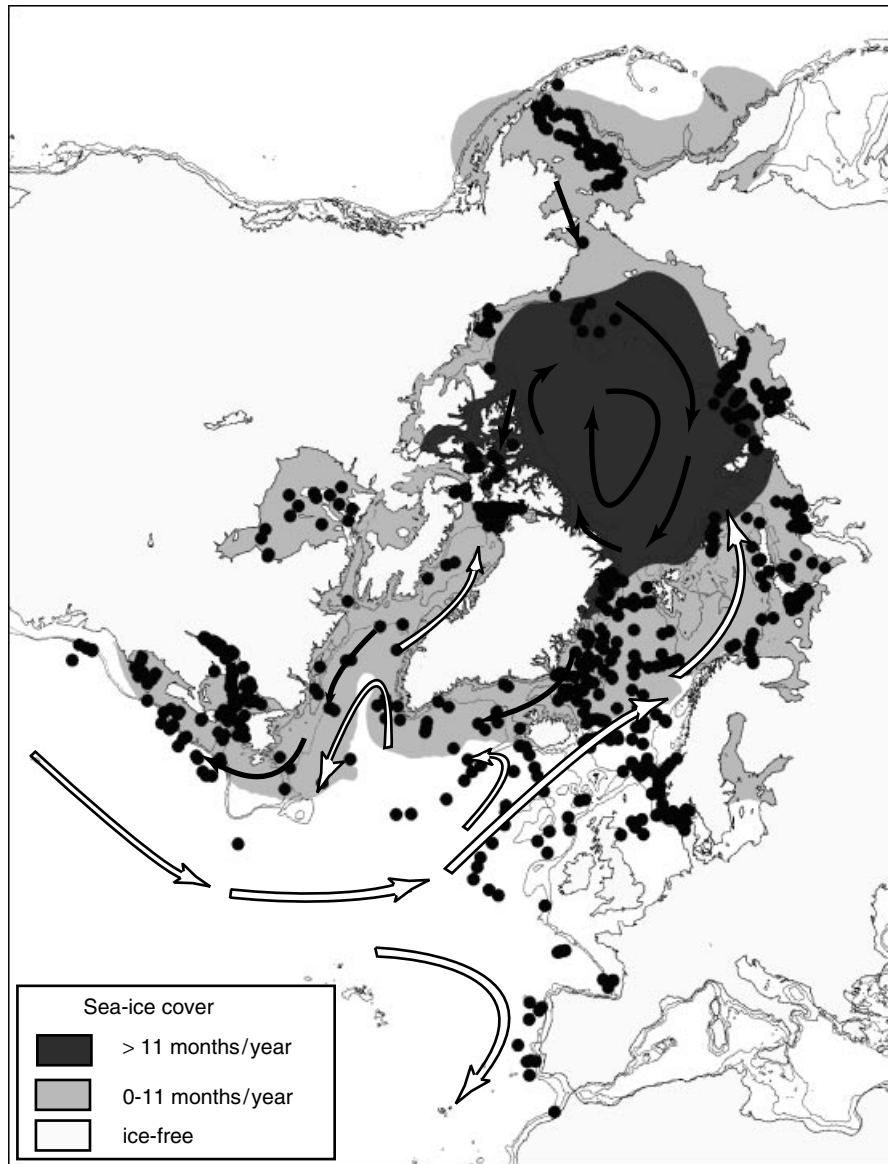


Figure 1 Map showing the location of reference sites (dots), the main sea-ice limits and surface currents. The dark grey zone corresponds to quasi-perennial sea-ice with more than 11 months/yr⁻¹ of sea-ice cover greater than 50% and the light grey zone illustrates the area occupied by 0–11 months/yr⁻¹ of sea-ice. The isobaths correspond to 200 and 1000 m water depth. The arrows illustrate schematically the surface currents in the North Atlantic and adjacent polar seas (white arrows for warm currents from the south, and black arrows for cold currents)

with the almost complete disappearance of processes. Other specimens of *O. centrocarpum* have been assigned to an Arctic morphotype (Fig. 3). This morphotype is relatively frequent and shows a morphology intermediate between *O. centrocarpum* sensu Wall & Dale 1966 and *O. centrocarpum* morphotype *cezare*. It is distinguished by processes that are imperfectly developed and has a distribution that is of low density. It corresponds to *O. centrocarpum* type B described from the Champlain Sea sediment (de Vernal *et al.*, 1989). The Arctic and *cezare* morphotypes probably represent morphological gradation of the same taxon. They seem to characterise Arctic and cold environments, whereas *O. centrocarpum* sensu Wall & Dale 1966 appears more ubiquitous (Fig. 3). Although these morphotypes were distinguished in the raw data base, they remain grouped for statistical treatment for two main reasons. First, the $n = 371$ data base (Rochon *et al.*, 1999) may include specimens belonging to the Arctic and *cezare* morphotypes of *Operculodinium centrocarpum* that were overlooked when initial counts were made. Second, because the morphological variations of *Operculodinium centrocarpum* are gradational, the identification of various

morphotypes is a rather subtle and subjective matter, and it would be impossible to ensure consistency in relative counts from one analyst to another. Thus, although the morphological variations in *O. centrocarpum* very probably have ecological significance, we have grouped all morphotypes together for data treatments (cf. Table 1). It must be noted finally that we use the name *O. centrocarpum* not in the strict sense but according to Quaternary palynological custom. *Operculodinium centrocarpum* was first described from the Miocene of Australia (Deflandre and Cookson, 1955) and is larger and more robust than Quaternary forms (Head, 1996b; Rochon *et al.*, 1999).

Spiny round brown cysts occur frequently in our high-latitude assemblages and represent another taxonomically problematic group. These cysts are referred to as *Algidasphaeridium? minutum* var. *minutum* and *Algidasphaeridium? minutum* var. *cezare* in the $n = 371$ data base (Rochon *et al.*, 1999), and respectively as *Islandinium minutum* and *Islandinium? cezare* in the present work, following Head *et al.* (this issue). A third species, *Echinidinium karaense*, also occurs in our high-latitude assemblages (Head *et al.*, this issue), and is

Table 1 List of dinocyst taxa systematically counted and reported in the raw $n = 677$ data base under four-letter codes. A total of 30 taxa (codes in bold) are used for statistical treatment. Some of these taxa result from grouping as indicated by notes in the table. The arrows point to taxa occurring currently in Arctic and sub-Arctic seas for which the distribution is illustrated in Figs 2–5 and Plate 2

Taxa	Code	Notes
cf. <i>Alexandrium tamarense</i> type cyst	Alex	
<i>Ataxiodinium choane</i>	Atax	
<i>Bitectatodinium tepikiense</i>	Btep	
<i>Impagidinium aculeatum</i>	Iacu	
<i>Impagidinium pallidum</i>	→ Ipal	
<i>Impagidinium paradoxum</i>	Ipar	
<i>Impagidinium patulum</i>	Ipat	
<i>Impagidinium sphaericum</i>	Isph	
<i>Impagidinium striatum</i>	Istr	
<i>Impagidinium</i> spp.	Ispp	
<i>Lingulodinium machaerophorum</i>	Lmac	
<i>Nematosphaeropsis labyrinthus</i>	→ Nlab	
<i>Operculodinium centrocarpum</i> sensu Wall & Dale 1966	→ Ocen	
<i>O. centrocarpum</i> sensu Wall & Dale 1966 - short processes	Ocss	Grouped with <i>O. centrocarpum</i> sensu Wall & Dale 1966
<i>Operculodinium centrocarpum</i> - Arctic morphotype	→ Oarc	Grouped with <i>O. centrocarpum</i> sensu Wall & Dale 1966
<i>Operculodinium israelianum</i>	Oisr	
<i>Operculodinium cf. janduchenei</i>	Ojan	
<i>Operculodinium centrocarpum</i> - morphotype <i>cezare</i>	Ocez	Grouped with <i>O. centrocarpum</i> sensu Wall & Dale 1966
<i>Pyxidinosia reticulata</i>	Pret	
<i>Spiniferites membranaceus</i>	Smem	
<i>Spiniferites delicatus</i>	Sdel	Grouped with <i>S. membranaceus</i>
<i>Spiniferites elongatus</i>	→ Selo	
<i>Spiniferites ramosus</i>	Sram	
<i>Spiniferites belerius</i>	Sbel	Grouped with <i>S. membranaceus</i>
<i>Spiniferites bentorii</i>	Sben	
<i>Spiniferites bulloideus</i>	Sbul	Grouped with <i>S. ramosus</i>
<i>Spiniferites frigidus</i>	Sfri	Grouped with <i>S. elongatus</i>
<i>Spiniferites lazus</i>	Slaz	
<i>Spiniferites mirabilis-hyperacanthus</i>	Smir	
<i>Spiniferites</i> spp.	Sspp	
Cyst of <i>Pentapharsodinium dalei</i>	→ Pdal	
<i>Islandinium minutum</i>	→ Amin	
<i>Islandinium? cezare</i>	→ Amic	
<i>Echinidinium karaense</i>	Aspp	Grouped with <i>Islandinium? cezare</i>
<i>Brigantedinium</i> spp.	→ Bspp	
<i>Brigantedinium cariacense</i>	Bcar	Grouped with <i>Brigantedinium</i> spp.
<i>Brigantedinium simplex</i>	Bsim	Grouped with <i>Brigantedinium</i> spp.
Protoperidinioids	Peri	
<i>Lejeunecysta sabrina</i>	Lsab	Grouped with Protoperidinioids
<i>Lejeunecysta oliva</i>	Loli	Grouped with Protoperidinioids
<i>Selenopemphix nephroides</i>	Sele	
<i>Xandarodinium xanthum</i>	Xand	Grouped with Protoperidinioids
<i>Selenopemphix quanta</i>	→ Squa	
Cyst of <i>Protoperidinium nudum</i>	Pnud	Grouped with <i>S. quanta</i>
<i>Trinovantedinium appianatum</i>	Tapp	
<i>Trinovantedinium variabile</i>	Tvar	
<i>Votadinium calvum</i>	Vcal	Grouped with Protoperidinioids
<i>Votadinium spinosum</i>	Vspi	Grouped with Protoperidinioids
Cyst of <i>Protoperidinium americanum</i>	Pame	
<i>Quinquecuspsis concreta</i> ^a	Qcon	
Cyst of <i>Polykrikos schwartzii</i>	Psch	
Cyst of <i>Polykrikos</i> sp.-Arctic morphotype ^a	→ Parc	
Cyst of <i>Polykrikos kofoidii</i> ^a	Pkof	

^a Not recorded in the $n = 371$ data base.

distinguished from *Islandinium? cezare* principally by subtle differences in process morphology. *Echinidinium karaense* was not distinguished from *Islandinium? cezare* in the $n = 371$ data base (Rochon *et al.*, 1999), and although it is included in the

$n = 677$ data base, it cannot be used separately in the present statistical analyses. Here, we use the name *Islandinium? cezare* sensu lato when referring collectively to *Islandinium? cezare* sensu stricto and *Echinidinium karaense*.

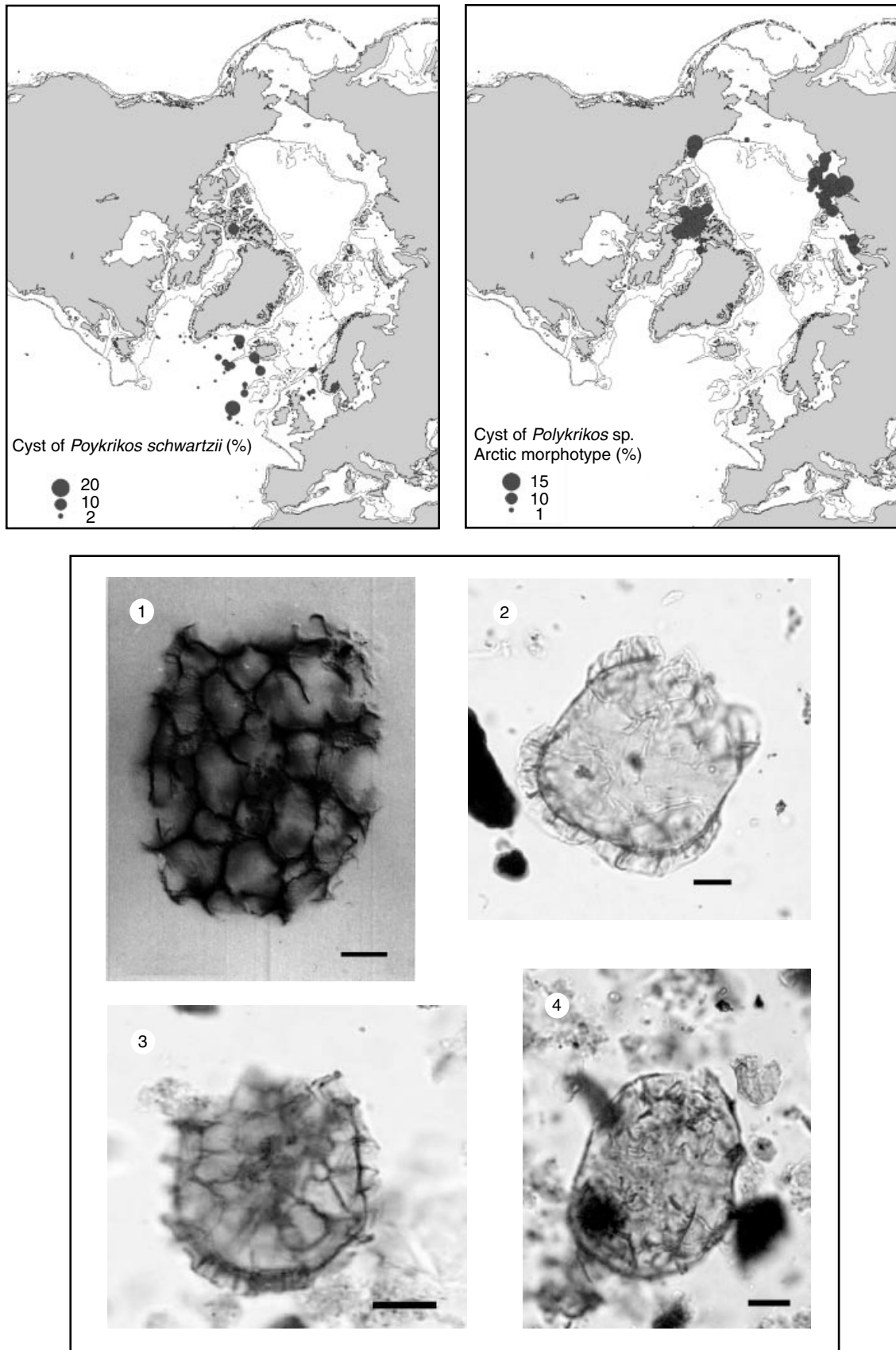


Figure 2 Distribution maps of the percentages of cysts of *Polykrikos schwartzii* (upper left panel) and *Polykrikos* sp. Arctic morphotype (upper right), and illustration of representative cyst specimens (lower panel). (1) Cyst of *Polykrikos schwartzii* as figured in Harland, 1981, 1983, Firth of Forth (Scotland), specimen MPK2600. (2) Cyst of *Polykrikos* sp. Arctic morphotype: Core 9722-05B (0–1 cm), UQP 1246-3, M31/1. (3) Cyst of *Polykrikos* sp. Arctic morphotype: Core 9722-01E (0–1 cm), UQP 1246-6, E29/1. (4) Cyst of *Polykrikos* sp. Arctic morphotype: Core 9722-01E (0–1 cm), UQP 1246-6, C39/3-4. Scale bars on the photographs are 10 µm

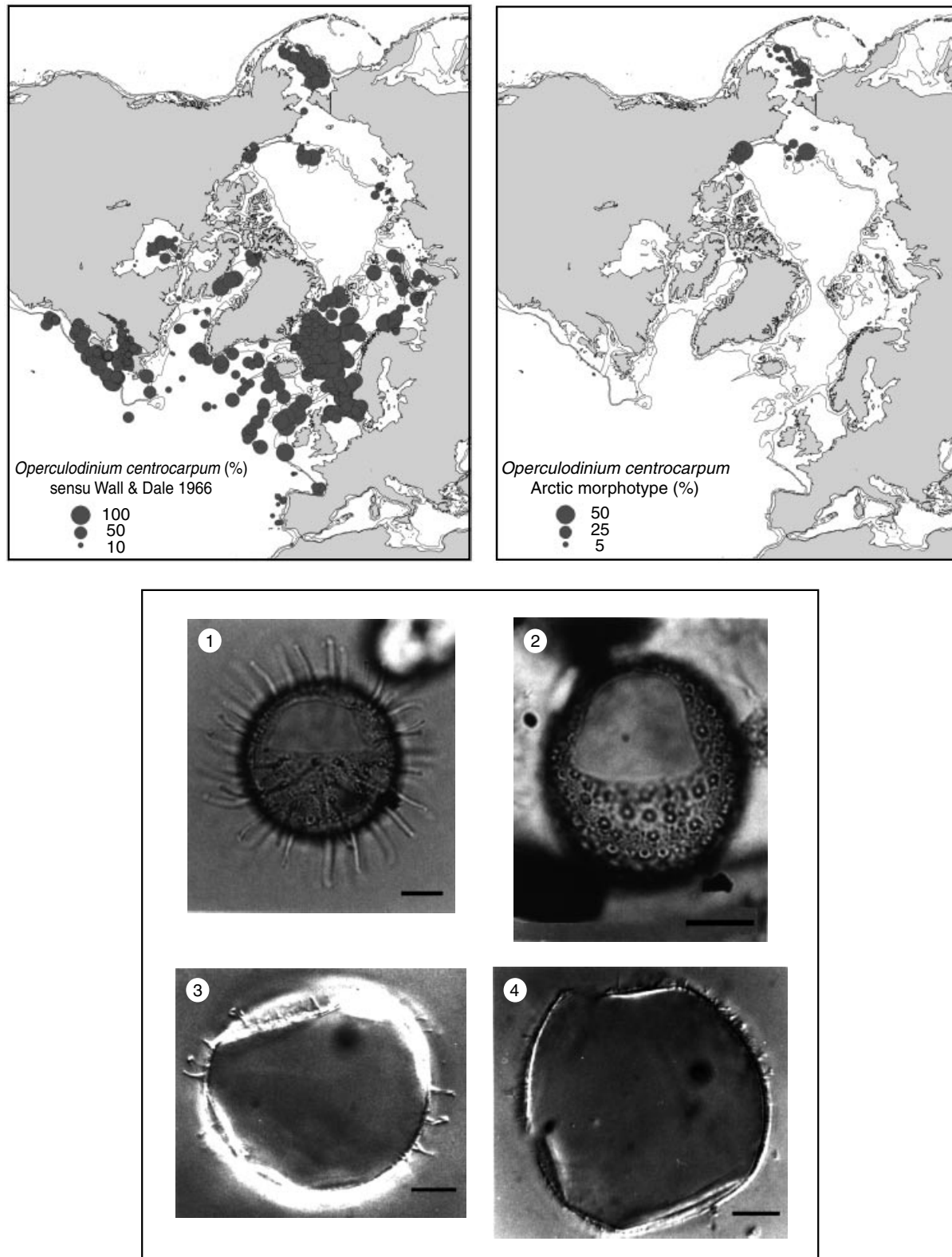


Figure 3 Distribution maps of the percentages of *Operculodinium centrocarpum* sensu Wall & Dale 1966 (upper left panel) and *Operculodinium centrocarpum* Arctic morphotype (upper right panel), and illustration of the respective morphology of the different morphotypes (lower panel). (1) *Operculodinium centrocarpum* sensu Wall and Dale 1966: slide HU-90-013-006, UQP 482-3, E26/4. (2) *Operculodinium centrocarpum*—short processes form: slide HU-90-013-017 (0–1 cm), UQP 482-6, N25/4. (3) *Operculodinium centrocarpum* Arctic morphotype (type B of de Vernal *et al.*, 1989), from Saint-Césaire, Champlain Sea, Quebec, UQP 200-6B, M47/2. (4) *Operculodinium centrocarpum* morphotype *cezare*, from Saint-Césaire, Champlain Sea, Quebec, UQP 200-6B, O44/0. Scale bars on the photographs are 10 µm

Most surface sediment samples included in the data base were collected by box or gravity coring and correspond to the top first centimetre of sediment. Samples from piston core were not used because the surface sediment is often missing. In case of doubt concerning the 'recent' age of the surface sediment,

samples were discarded from the data base. More information concerning the sampling and sediment characteristics can be found in Rochon *et al.* (1999) and manuscripts reporting on regional data sets (Kunz-Pirrung, 1998; this issue; Radi *et al.*, this issue; Voronina *et al.*, this issue; Hamel, 2001; Mudie

and Rochon, this issue; Grøsfjeld and Harland, this issue). The systematic identification and count of dinocysts was performed by scanning at least three randomly distributed horizontal fields on the palynological slides. The number of fields scanned was determined depending upon the concentration of dinocysts in the slide. Ideally, a scan was done until a sum of at least 400 specimens was reached. In samples containing sparse assemblages, the entire slide was scanned. On average, 400 specimens were identified and counted in each sample. However, lower counts were performed for many samples; among the 677 samples retained in the data base, 40 have counts ranging 25–100. The raw dinocyst counts include 53 taxa, among which 30 were used for statistical treatment after grouping (cf. Table 1). The raw dinocyst counts and percentages of the 30 taxa selected in the 677 surface sediment samples of the updated data base presented here can be found on the websites of GEOTOP (<http://www.geotop.uqam.ca/>) and the PANGAEA data bank of the Alfred Wegener Institute for Polar and Marine Research (<http://www.pangaea.de>).

The hydrographic data

Sea-ice cover was compiled from data provided by the National Climate Data Center (NCDC) in Boulder, Colorado, comprising measurements for a 1° by 1° grid and spanning 1953 to 1990. Mean sea-ice cover is expressed here as the number of months per year with sea-ice concentration greater than 50% (see also de Vernal and Hillaire-Marcel, 2000; Plate 1). It should be noted that the NCDC data cover most of the Northern Hemisphere except for a few marine basins such as the Okhotsk Sea and the Estuary and Gulf of St Lawrence. In the case of the Estuary and Gulf of St Lawrence, the sea-ice data are from Markham's (1980) atlas and consist of a compilation after a couple of years of observation.

Sea-surface (0 m depth) temperature and salinity are compiled from data published as CD-ROMs by the National Ocean Data Center (NODC, 1994). For most sites, simple averages were calculated from all values included within a radius of 30 nautical miles around the sites. A radius of 60 nautical miles was used in areas where instrumental measurements are sparse (<2). In the North Atlantic Ocean and adjacent subpolar seas, hydrographic data are abundant enough to develop an accurate data base that includes the mean and standard deviation for sea-surface temperature and salinity for the coldest and warmest months, i.e. February and August.

In the Arctic domain, the establishment of the reference hydrographic data base is problematic because measurements are extremely sparse in many areas, and multiyear synoptic data are rare. In many instances, data are too scattered, even at a radius of 60 nautical miles, to obtain a sensible average. In such cases, the extrapolated data fields for sea-surface temperature and salinity provided by NODC (1994) are used instead of compiled data. For a few Arctic sites, it was possible to compare means from instrumental data and the extrapolated data fields. As for the sea-surface temperature in August, both extrapolated and actual data yield consistent information within the range of interannual variability. However, regarding the sea-surface salinity in August, data revealed extremely variable conditions from one year to another, and the comparison of means with extrapolated data fields revealed large discrepancies at many sites, especially in the low-salinity (<30) domain. This is particularly critical in the Canadian Arctic Archipelago, where data are extremely sparse (cf. Mudie and Rochon, this issue). By default, we have used the extrapolated data fields for sea-surface salinity at most

sites from the Arctic seas, i.e. where no data are available, or where there is too large an uncertainty owing to low numbers of measurements and a large standard deviation around the average ($\sigma > 5$). We also excluded from the data base all sites with salinity below 17, occurring in nearshore and shallow environments because of too large variability or uncertainty in actual hydrographic conditions. This omission unfortunately constrains the use of the data base for reconstructions in Arctic estuarine environments or their late-glacial analogues.

In the Arctic domain, data for the coldest month (February) are particularly rare and, for many areas, no extrapolated data field is available. In the event of no data availability, we have used an extrapolated value. We have assumed temperature at the freezing point in February in as much as the sites are occupied by extensive winter sea-ice, and we have used the overall relationship between winter and summer salinity to make salinity estimations.

In addition to the NODC data sets published in 1994, there are hydrographic data available on regional scales, which could have been used locally in some instances. These data are important for validating the estimates obtained in new study areas (see Mudie and Rochon, this issue). However, in order to keep the hydrographic data base internally consistent, we have preferred to use the compiled data or extrapolated data field provided by NODC (1994). The only exception is the Estuary and Gulf of St Lawrence area, which is not covered by NODC (1994) and where very large numbers of hydrographic measurements were made until 1990 (data provided by the Department of Environment-Canada), allowing reliable compilation.

There also are uncertainties with respect to the time interval that is respectively represented by the hydrographic measurements and by microfossil assemblages in the surface sediment sample. The hydrographic data correspond to averages established after measurements made during the last decades, whereas the dinocyst spectra from surface sediment samples may include populations representative of a couple of years to a millennium depending upon the sedimentation rate and the biological mixing depth at the sampling sites. This is a problem common to all 'modern' geochemical or micropalaeontological data bases established from surface sediment samples.

The overall temperature, salinity and sea-ice cover domains represented in the $n = 371$ and $n = 677$ data bases are illustrated in Fig. 4. Tables reporting the mean sea-ice cover, temperature (August and February) and salinity (August and February) with standard deviations when available are archived on the websites of GEOTOP (<http://www.geotop.uqam.ca/>) and the data bank PANGAEA of the Alfred Wegener Institute for Polar and Marine Research (<http://www.pangaea.de>).

Relationships between dinocyst assemblages and hydrographic data with special attention to the Arctic domain

The updated dinocyst data base includes data from mid- to polar northern latitudes. The distribution of assemblages in the northern North Atlantic Ocean has been documented previously (de Vernal *et al.* 1997; Rochon *et al.*, 1999) and here we focus mostly on assemblages specific to the polar domain. In general, the species diversity is much larger in assemblages from lower latitudes than from Arctic environments. Of the 30 taxa retained within the updated

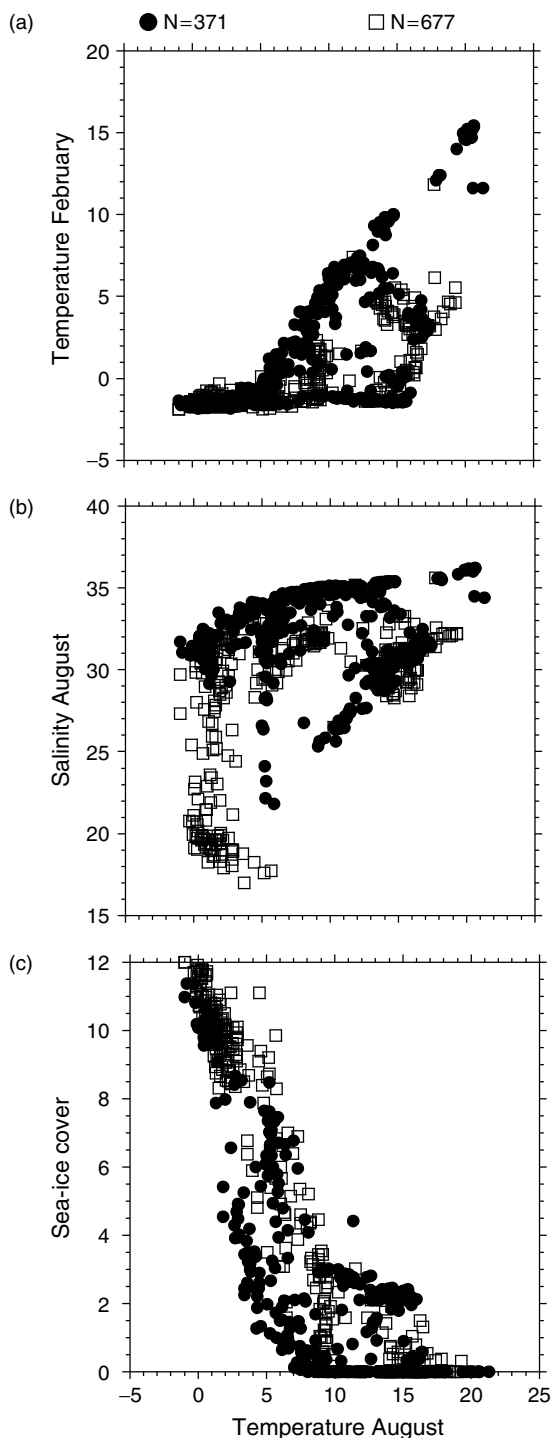


Figure 4 Relationships between sea-surface temperature in August and sea-surface temperature in February (a), sea-surface salinity in August (b) and sea-ice cover (c). The circles correspond to references sites of the 'n = 371' data base as published by de Vernal *et al.* (1997) and Rochon *et al.* (1999), whereas the squares correspond to the additional reference sites included in the 'n = 677' data base (see Plate 1). Temperature is in degree celsius and sea-ice cover in months/year

n = 677 data base, only 11 are frequent in the Arctic seas (Figs 2, 3, 5 and 6, and Plate 2).

Some of the taxa occurring in the Arctic seas are cosmopolitan and appear to tolerate a wide range of environmental conditions. *Operculodinium centrocarpum* sensu Wall & Dale 1966 is particularly ubiquitous, although morphological variations in Arctic environments (see *Operculodinium*

centrocarpum Arctic morphotype; Fig. 3) might be associated with phenotypes adapted to low salinity and cold environments, or to reduced season of growth and light levels. *Brigantedinium* spp. is another taxon that seems to be particularly cosmopolitan, especially in epicontinental environments (Fig. 5 and Plate 2). Its distribution does not show any preference with regard to temperature or salinity, nor with nutrient availability or productivity (Devillers and de Vernal, 2000). It probably is an opportunistic genus. The cyst of *Pentapfarsodinium dalei* is another ubiquitous taxon, but it seems to be more specific of sub-Arctic environments and has limited occurrence in the coldest polar regions (Fig. 6 and Plate 2).

Other cosmopolitan taxa have limited occurrence in the coldest Arctic seas. For example, *Nematosphaeropsis labyrinthus* and *Spiniferites elongatus* are ubiquitous in middle-high latitudes, but they show some preference for open oceanic environments in the temperate to subpolar domains. *Selenopemphix quanta* also shows preference for the temperate to subpolar domain, and occurs mainly in neritic environments where salinity can be relatively low (Fig. 5 and Plate 2).

There are, however, taxa that are apparently more specific to Arctic and sub-Arctic seas. This is the case of *Islandinium minutum*, and more especially *Islandinium? cezare* s.l., which are abundant mainly in assemblages of the continental margins where seasonal sea-ice cover is a conspicuous feature (Head *et al.*, this issue; Fig. 5 and Plate 2). The polar taxa also include *Impagidinium pallidum*, recorded as having maximum occurrence in the Greenland Sea, where surface waters are cold and characterised by relatively high salinity (Fig. 6 and Plate 2), and finally, the cyst of *Polykrikos* sp. Arctic morphotype, which occurs almost exclusively in shelf environments of the Canadian Arctic and Laptev and Kara seas (Fig. 2).

Principal component analysis was performed after logarithmic (ln) transformation of percentage data for the 30 taxa selected using the software of Guiot and Goeury (1996). A logarithmic transformation is useful in as much as the dominant taxa are often cosmopolitan, whereas accompanying taxa generally have more specific environmental requirements and more restricted distributions. The first principal component (PC1), which explains 48.9% of the total variance, shows an opposition between the polar taxa, including the cyst of *Polykrikos* sp. Arctic morphotype, *Islandinium minutum*, *Islandinium? cezare* s.l., *Brigantedinium* spp. and *Impagidinium pallidum* on one side, and most other taxa on the other side (Fig. 7). Scores of the first component reveal a distribution closely related to latitudinal gradients and water mass boundaries (Plate 3a), positive values being related to open ocean temperate-subpolar waters, and negative values corresponding to Arctic seas and areas that are marked by polar currents and extensive sea-ice. Actually, PC1 correlates positively with the temperature of August ($R = 0.802$) and February ($R = 0.798$) and with salinity ($R = 0.559$), whereas it correlates negatively with the sea-ice cover ($R = 0.728$) according to linear regression. Better fits can be obtained with polynomial of order 2 or 3 relationships. The second component (PC2) explains 22.2% of the variance and corresponds to an opposition between both Arctic and temperate taxa on one side, and taxa cosmopolitan in the sub-Arctic domain, such as the cyst of *Pentapfarsodinium dalei*, *Spiniferites elongatus* and *Operculodinium centrocarpum*, on the other side. The geographical distribution of PC2 scores shows no relationship with temperature or salinity (Plate 3b). It probably is related to the distribution of another parameter, which could be linked, for example, to productivity, nutrient distribution or the trophic structure of planktonic populations (see also Devillers and de

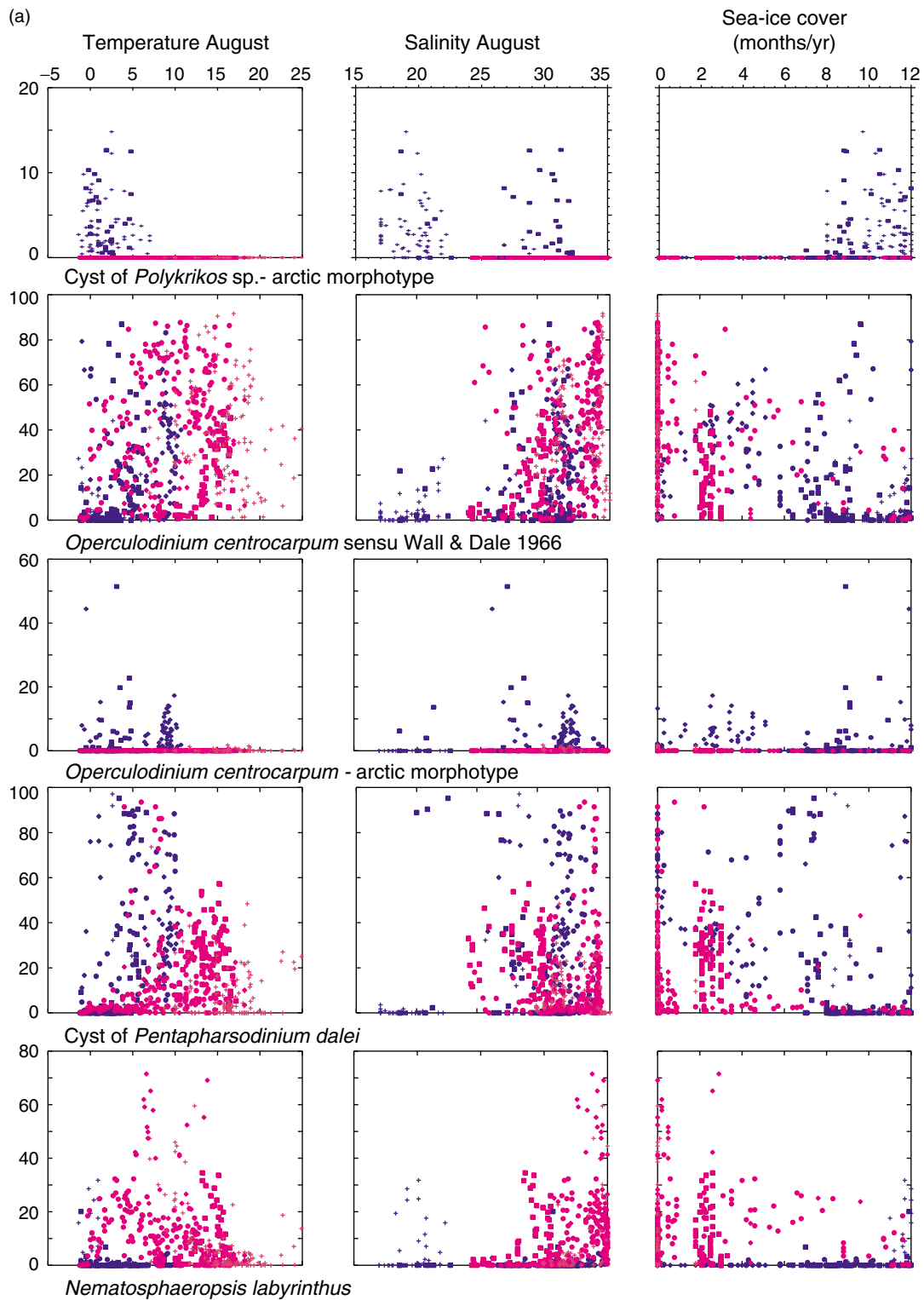


Plate 2 Relationships between the percentages of the main dinocyst taxa occurring in the Arctic seas and the August sea-surface temperature and salinity, and the sea-ice cover. The distribution of the percentages of the other North Atlantic taxa (cf. Table 1) as illustrated in de Vernal *et al.* (1997) and Rochon *et al.* (1999) from the $n = 371$ data base is basically unchanged. In the $n = 677$ data base, the distribution of the additional taxa such as the cyst of *Polykrikos kofoidii* and *Quinquecuspsis concreta* is restricted to the Bering Sea (for information on their regional distribution, see Radi *et al.*, this issue). The geographical location of the spectra is indicated as follows: blue indicates data from the Arctic seas (squares = Canadian Arctic, including Beaufort Sea, Hudson Bay, Baffin Bay, and the Canadian Archipelago Channels; circles = Barents Sea; crosses = Kara Sea and Laptev Sea; diamonds = western Arctic, including the Chukchi Sea and the Siberian Sea), and red indicates data from the North Atlantic Ocean and adjacent basins (squares = Estuary and Gulf of St Lawrence; circles = Norwegian–Greenland seas; crosses = southeastern Canadian and eastern American margins; diamonds = all other sites from northwest to northeast North Atlantic)

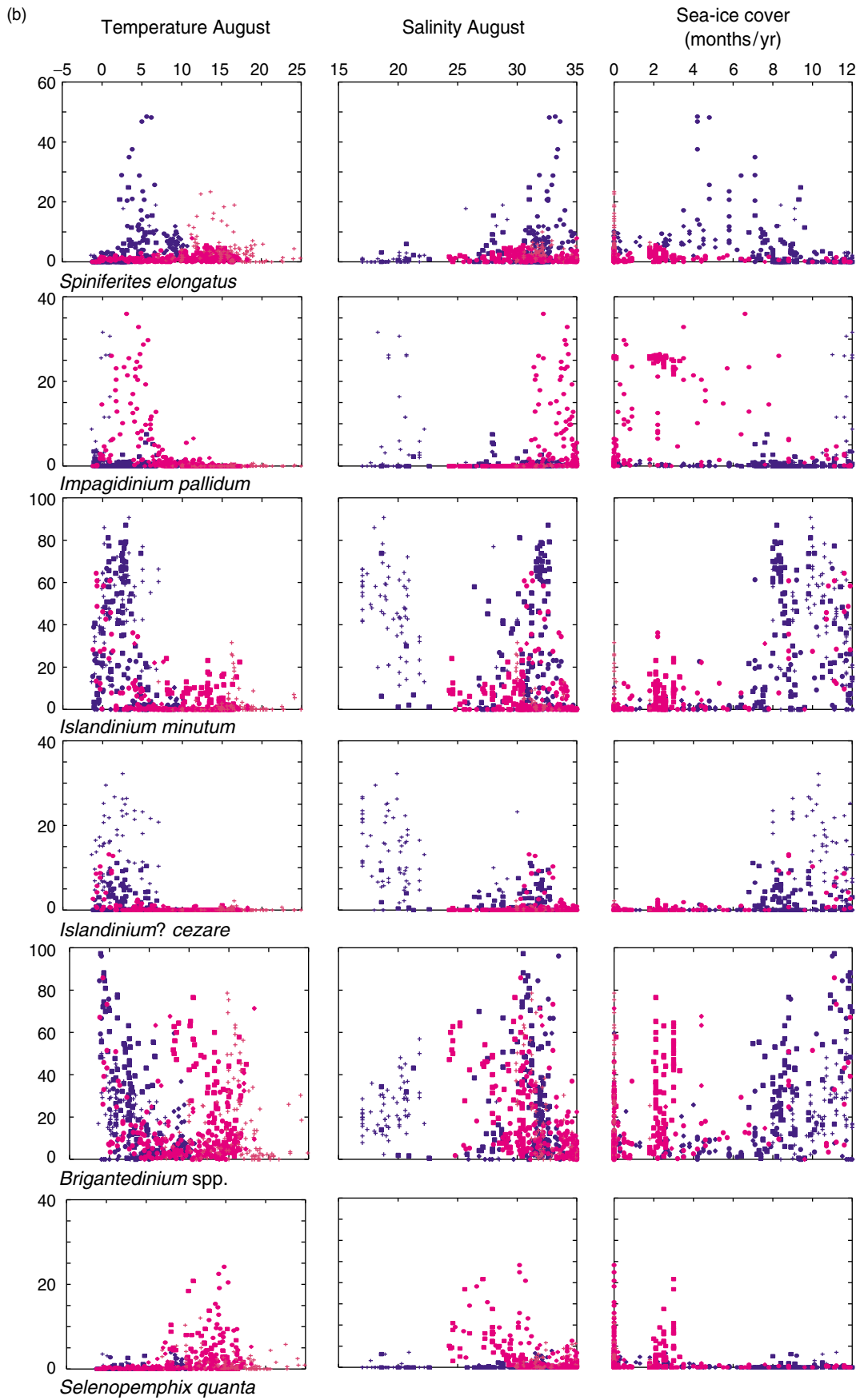


Plate 2 (Continued)

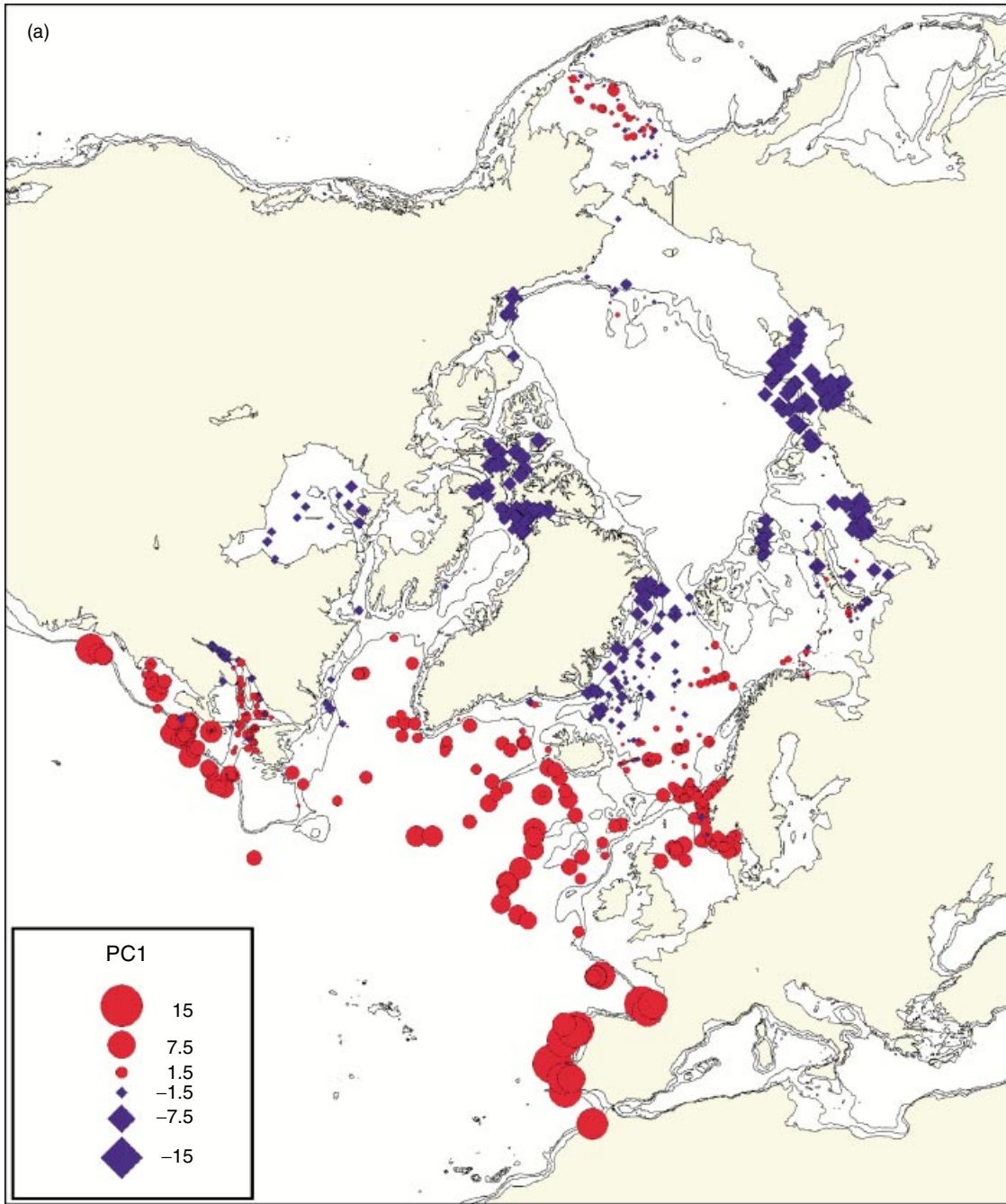


Plate 3 Geographical distribution of PC1 (a) and PC2 (b), which represent 48.9 and 22.2% of the total variance respectively. The principal component analysis was done on logarithmic values of the relative frequency of taxa expressed in per mil, using the software of Guiot and Goery (1996)

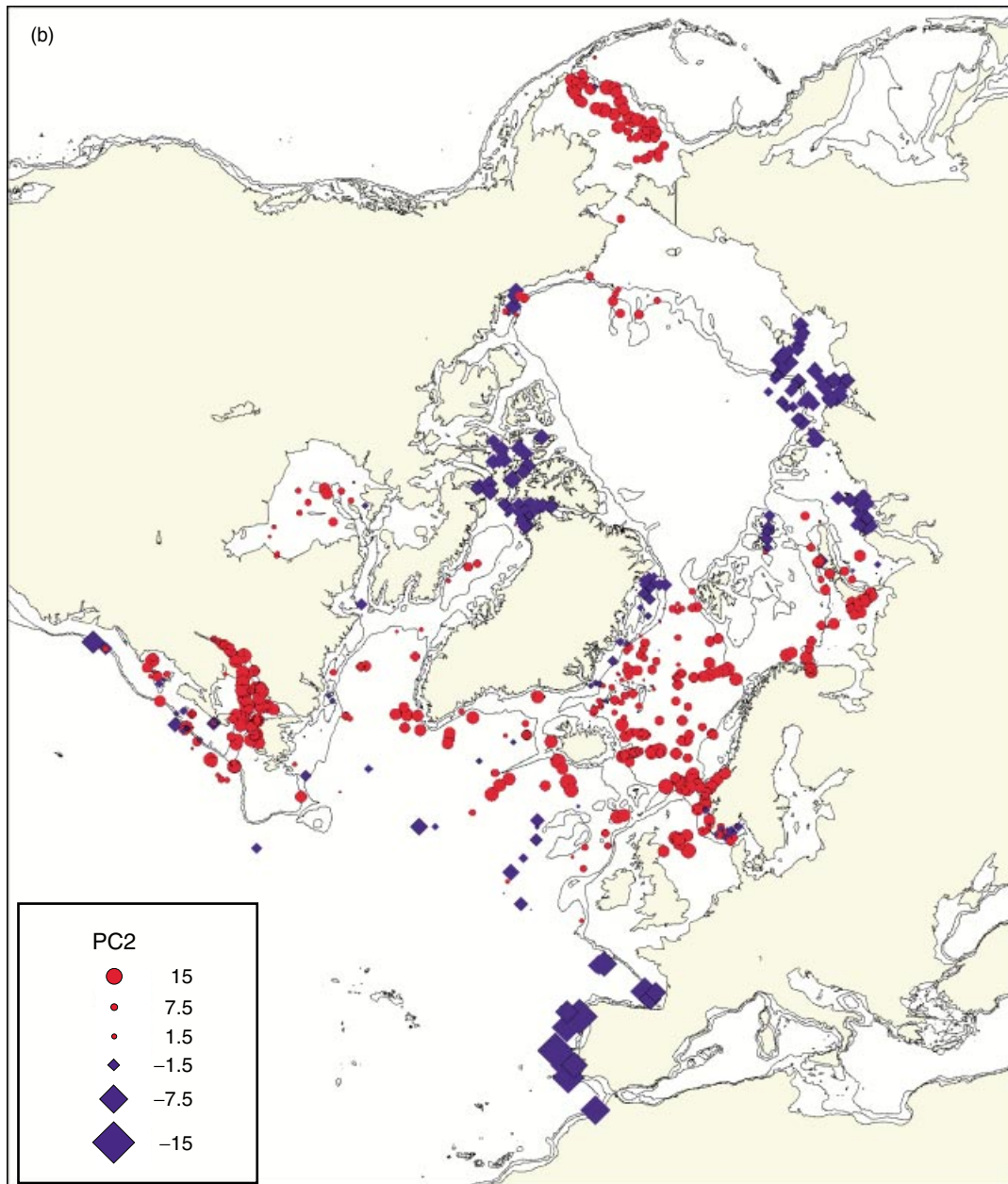


Plate 3 (Continued)

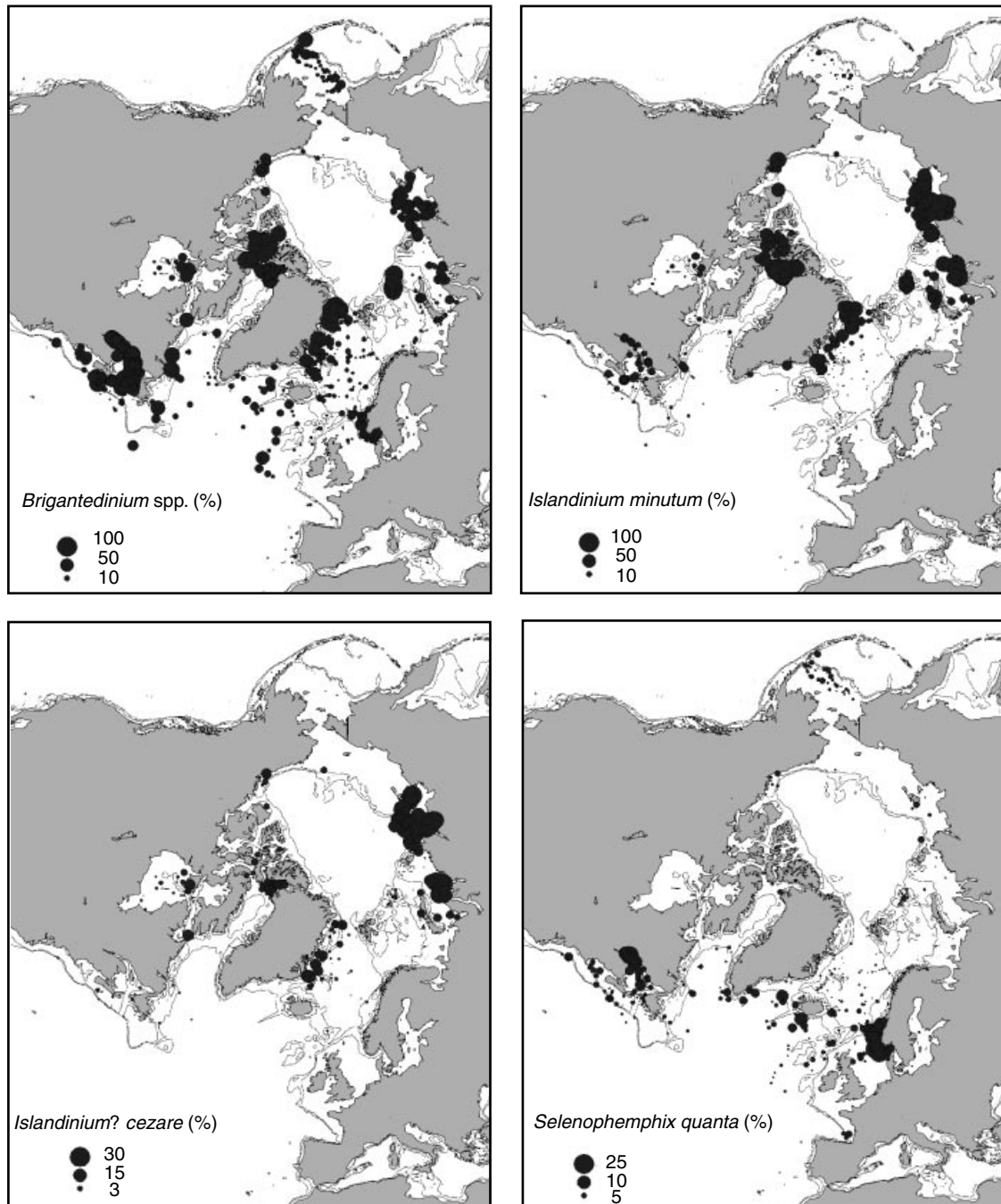


Figure 5 Distribution maps of the percentages of *Brigantedinium* spp. (upper left panel), *Islandinium minutum* (upper right panel), *Islandinium? cezare* s.l. (lower left panel) and *Selenopemphix quanta* (lower right panel).

Vernal, 2000). As a matter of fact, all taxa with negative loading of both PC1 and PC2 belong to the Polykrikaceae (cyst of *Polykrikos* sp.) or Protoperidiniaceae (*Brigantedinium* sp. and *Islandinium minutum*), which relate to a heterotrophic rather than autotrophic productivity (e.g. Taylor, 1987; Head *et al.*, this issue).

Quantitative estimates of past sea-surface conditions based on the best-analogue method

Many techniques for quantitative reconstructions of past environmental conditions have been developed during the past

decades. They are based on multiple regression techniques (e.g. Imbrie and Kipp, 1971), modern analogue approaches (e.g. Hutson, 1980; Prell, 1985; Guiot, 1990; Pflaumann *et al.*, 1996; Waelbroeck *et al.*, 1998), or neural network methods (e.g. Malmgren and Nordlund, 1997; Peyron *et al.*, 1998, 2000). Tentative estimation of past sea-surface conditions based on dinocyst assemblages has been made using several approaches, including canonical regressions and variants of the modern analogue techniques (de Vernal *et al.*, 1994), and the artificial neural network technique (Peyron and de Vernal, this issue). The artificial neural network approach generally yields accurate reconstruction, but may give estimates outside the range of training data sets by extrapolation in the case of non-analogue situations, as is the case with regression techniques. In contrast, the analogue approach permits identification of non-analogue situations and avoids reconstruction

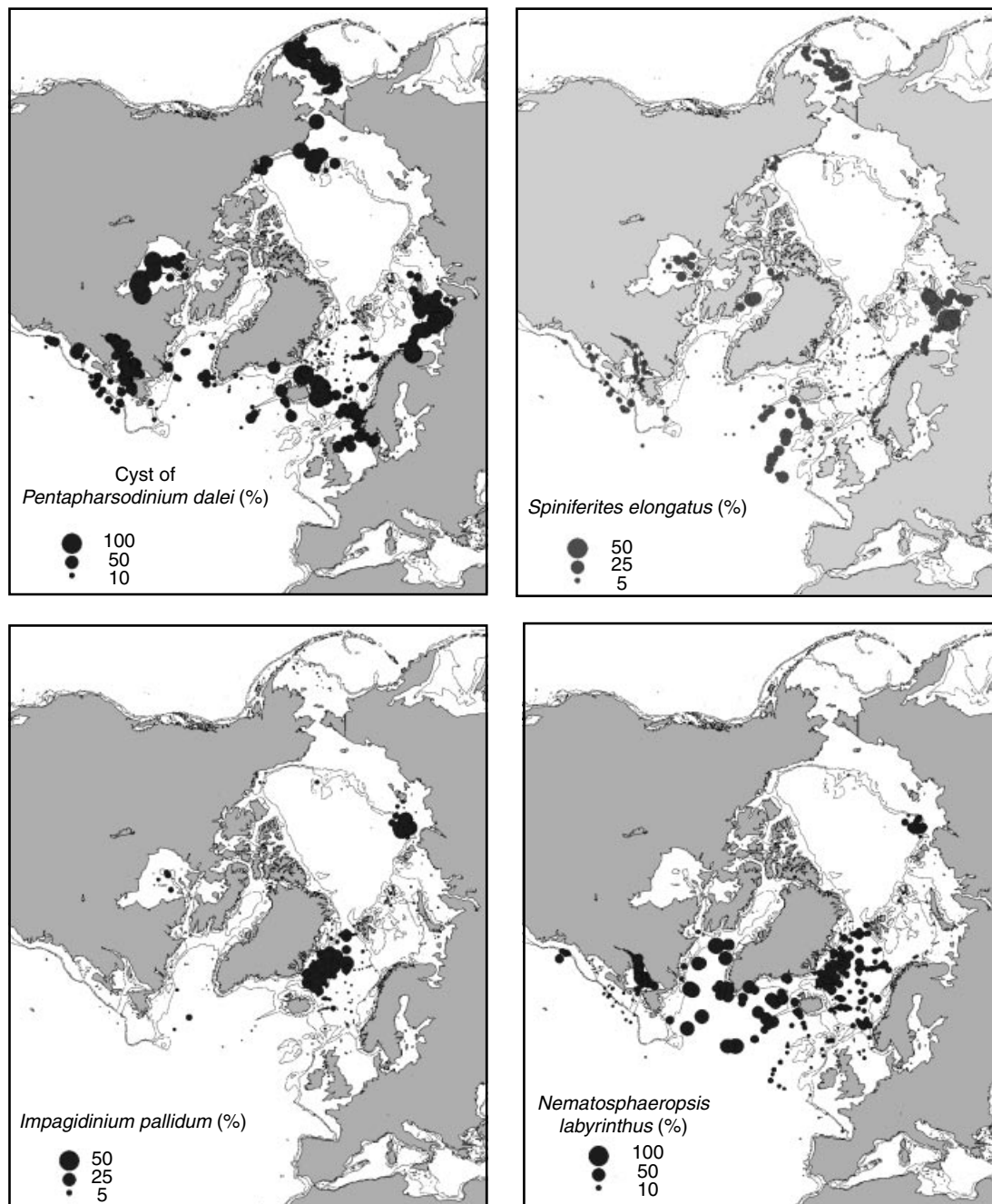


Figure 6 Distribution maps of the percentages of *Pentapharsodinium dalei* cysts (upper left panel), *Spiniferites elongatus* (upper right panel), *Impagidinium pallidum* (lower left panel) and *Nematospaeropsis labyrinthus* (lower right panel)

when the degree of uncertainty appears too high. Bootstrap neural network approaches also permit non-analogue situations to be identified, but in a less straightforward way. The artificial neural network method and its application for reconstructing past sea-surface parameters based on dinocyst data are fully developed by Peyron and de Vernal (this issue). Here, we present the procedure using the best-analogue technique that we adapted from the software of Guiot and Goeury (1996).

When developing a technique for quantitative estimates of a given parameter, a means to identify the most reliable procedure consists of validations, i.e. tests to quantify how accurately a given technique yields a reconstruction; in this case one that matches present-day environmental conditions. Many validation exercises were performed using successive updates of the dinocyst data base (de Vernal *et al.*, 1993, 1994, 1997; Rochon *et al.*, 1999). From these exercises, it

appears that logarithmic transformation of percentages is most powerful for the identification of the best analogues with respect to hydrographic conditions. This is because dominant species in the assemblages generally are the most ubiquitous, whereas the accompanying taxa often have more narrow ecological affinities. In other words, the presence and relative occurrence of accompanying taxa appear to be most diagnostic of environmental conditions.

The procedure we have adapted from the Guiot and Goeury (1996) software, developed initially for the analyses of pollen data, includes a few adjustments. In particular, relative abundance is expressed per thousand, instead of per cent in order to deal with whole numbers and to avoid decimals, which yield negative values when they are logarithmically transformed. One (1) is added to the frequency of each taxon in order to deal with values greater than zero, and the relative frequencies of taxa range from 1 to 1000. Another minor

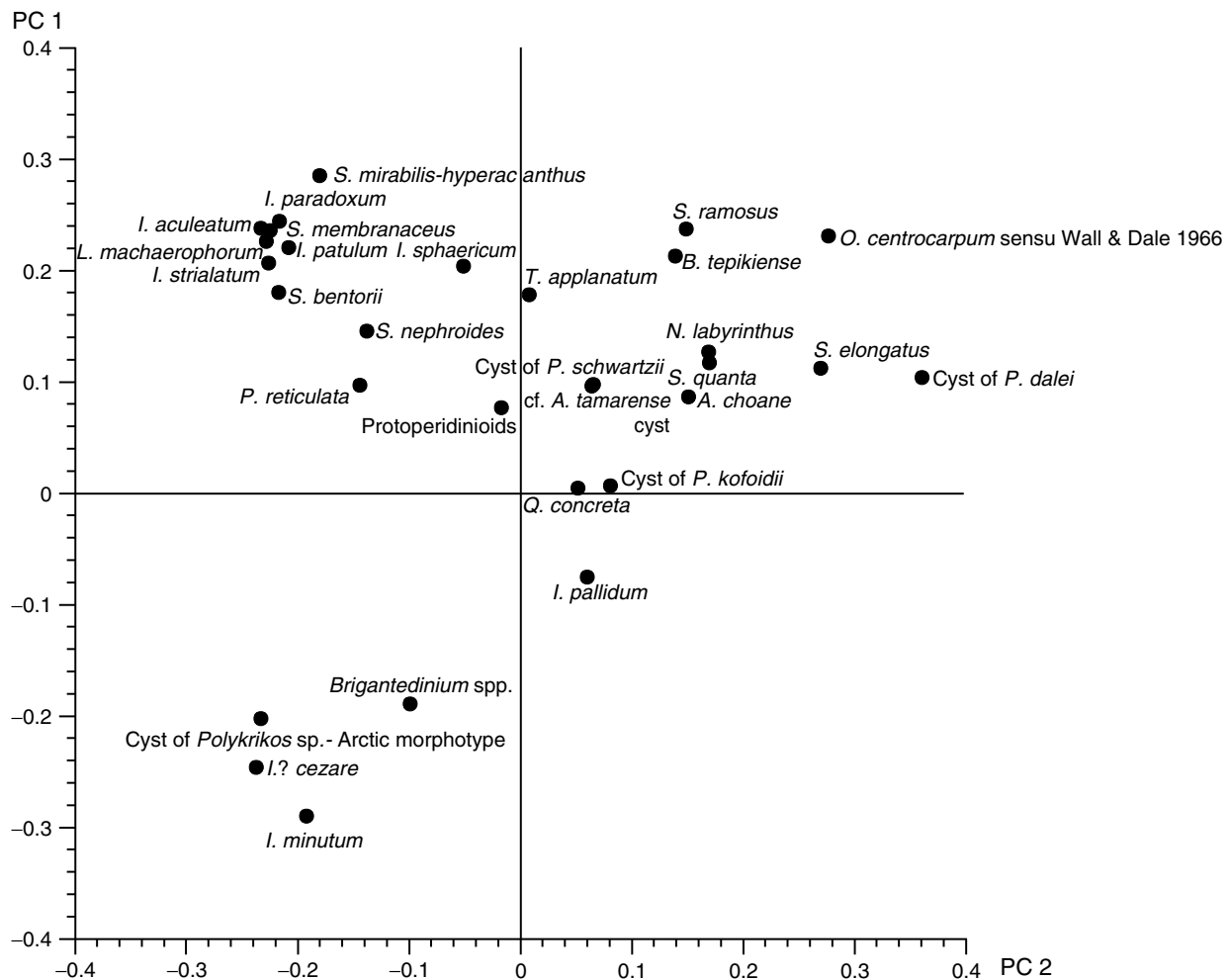


Figure 7 Loading of the 30 selected taxa in the 677 dinocyst assemblages of the reference dinocyst data base on the basis of the first two principal components

transformation consists of adjusting the frequency data ranging between 2 and 5 (i.e. 0.2 and 0.5%) to the value of 5 in order to make a better discrimination between absence (1) and presence (>5). This transformation is further justified because of the count limit, which occasionally is as low as 100 or 200 specimens. The zero elements are thus replaced by a value lower than the precision under which data were produced (cf. Kucera and Malmgren, 1998). After these transformations, the distance (d) between the spectrum to be analysed (t) and the spectra in the reference data base (i) is calculated based on the difference in relative frequency (f) for each taxon ($j = 1-30$) as follows

$$d = \sum_{j=1}^m W_j^2 [\ln f_{ij} - \ln f_{tj}]^2$$

In the above equation, W is a factor that may be used to weight the taxa. In the case of dinocyst assemblages, no weighting factor is used as we have not demonstrated from validation exercises that selectively weighting taxa on the basis of principal component analyses or on the basis of empirically defined ecological affinities can improve the accuracy of the reconstruction.

The distances calculated from the above equation permit us to select samples in the reference data base as best analogues. Here, we have searched for five analogues. The hydrographic data corresponding to these analogues are used to calculate an average that is weighted inversely to the distance of the analogues. This average constitutes the most probable estimates, and the results are reported within a confidence

interval defined from hydrographic data corresponding to these five best analogues. It is of note that a threshold value is defined on probabilistic grounds (i.e. a Monte-Carlo approach) in order to identify a non-analogue or poor-analogue situation. If the distance of the closest analogue is higher than the threshold calculated, no reconstruction is made. In the case of the $n = 677$ data base, the distance between pairs randomly taken in the data base averages 95.51, with a standard deviation of 42.41. The average minus standard deviation gives a threshold distance below which we consider the similarity to be significant. In the case of the $n = 677$ data base, the threshold distance is thus 53.1. For comparison, the $n = 371$ data base led to the calculation of a mean random distance of 82.9 ± 36.4 for a threshold value of 46.5. The slightly lower threshold value for the $n = 371$ data base than for the $n = 677$ data base results from the smaller size of the matrix with respect to both number of taxa and number of spectra.

The validation exercise permits assessment of the degree of accuracy of sea-surface reconstruction (Plate 4). It is performed on each surface sample for which we seek the best five analogues excluding the sample itself. It enables one to test the coherency of the spectra versus hydrographic parameters. Such a technique, also called leaving-one-out may, however, result in an underestimation of the error compared with the split-sampling technique that involves random division of the data set (cf. Birks, 1995). The reconstruction of four parameters is illustrated in Plate 4: the sea-surface temperature of the coldest and warmest month (February and August), the salinity for August and the seasonal extent of sea-ice cover. These

parameters have been shown to be most determinant on the distribution of dinoflagellate populations and dinocyst assemblages. It is of note that other validation exercises were done using seasonal (i.e. winter and summer) or annual means of temperature and resulted in reconstructions not as accurate as the ones obtained for monthly temperature means for the warmest and coldest month. This points to the fact that the annual cycle of temperature undoubtedly exerts a determinant control on the dinoflagellates and their cyst distribution. Seasonality certainly plays a major role in the life cycle of dinoflagellates, i.e. on the duration of vegetative versus encysted stages. Seasonality can be viewed as the difference between the temperature of the warmest and coldest months, or as the length of the season during which metabolic activities are interrupted, notably because of limited light owing to sea-ice cover. This would explain why the seasonal duration of sea-ice cover is one of the parameters that can be best reconstructed using dinocyst assemblages.

From the validation exercises, the linearity of the relationship around a slope of one over one, and the coefficients of correlation between estimates and observations provide a first indication of the reliability of the approach (see Plate 4). The degree of accuracy of the reconstruction is further constrained by the standard deviation of the difference between estimates and observations, which also is referred to as the root mean square error of prediction (RMSEP), and would be the best way to assess the error rate and to compare methods (cf. ter Braak and van Dam, 1989; Malmgren *et al.*, 2001). As shown in Plate 4, the degree of accuracy or prediction error establishes at $\pm 1.3^\circ\text{C}$ and $\pm 1.8^\circ\text{C}$ for the temperature of February and August respectively, ± 1.8 for the salinity, and ± 1.5 months yr^{-1} for the sea-ice cover.

On the whole, the validation exercise for the $n = 677$ data base yields results that are similar to those of the validation made for the $n = 371$ data base (de Vernal *et al.*, 1997; Rochon *et al.*, 1999). However, in the case of the $n = 677$ data base, there is a larger error for salinity, particularly in the low salinity domain that corresponds primarily to data from the Canadian Arctic and the Russian Arctic. The apparently poor accuracy of salinity estimates in this domain can be explained by the high variability of this parameter and by the lack of accuracy of instrumental data (see above). Actually, about half the spread of estimated versus observed salinity values can be attributed to inaccurate hydrographic measurements. In summary, the validation exercises reveal high accuracy of the approach for the reconstructions of sea-surface conditions, although some reservation has to be exercised when reconstructing low salinity in Arctic environments.

Examples of application

Two examples, using the procedure described above with the $n = 371$ and $n = 677$ data bases, are treated here. The first example is based on a core collected from the northern Labrador Sea (HU-84-030-021; de Vernal and Hillaire-Marcel, 1987). The coring site is located in the northwestern part of the North Atlantic, a domain well represented by the $n = 371$ data base. The second example is from the Barents Sea (core PL96-112; Voronina *et al.*, this issue), at the northeastern limit of the area represented by the $n = 371$ data base. These two examples are selected because they represent distinct circum-Arctic areas. They also are selected because the sediments in both cores are characterised by abundant dinocysts, allowing statistically representative dinocyst counts.

The two examples illustrate the coherency or discrepancies of palaeoceanographic estimates resulting from the use of the two data bases and identify the strengths and weaknesses of the method.

The northwest North Atlantic

The sedimentary sequence of core HU-84-030-021 ($58^\circ 22.06'N$, $57^\circ 30.42'W$; water depth = 2853 m) spans the past 20 000 yr. The core was collected on the continental slope from the western Labrador Sea, where surface waters are under the influence of an eastern branch of the West Greenland Current (Fig. 8a). At the coring site, present-day mean sea-surface temperature is $3.5 \pm 0.4^\circ\text{C}$ and $6.8 \pm 1.05^\circ\text{C}$ in February and August respectively, and the

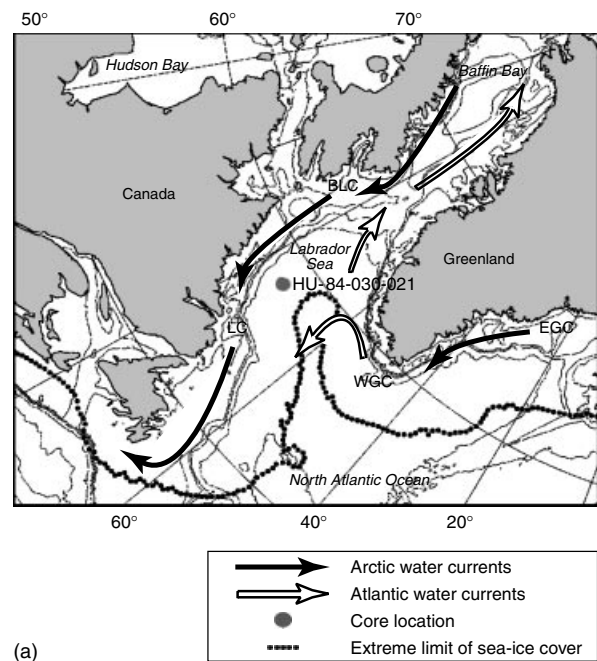


Figure 8 Core location and time series from the northwestern North Atlantic (core HU-84-030-021; $58^\circ 22.06'N$ - $57^\circ 30.42'W$; 2853 m) spanning the last 20 000 yr. (a) Location map for core HU-84-030-021 showing the surface water circulation pattern, with cold currents from the Arctic illustrated by black arrows (Baffin Land Current = BLC; Labrador Current = LC; East Greenland Current = EGC) and the warmer West Greenland Current (WGC) illustrated by white arrows. (b) Summary diagram of dinocyst assemblages for core HU-84-030-021. The chronological marks indicated in the left margins of the diagrams correspond to accelerator mass spectrometry (AMS) ^{14}C ages on planktonic foraminifers (*Neogloboquadrina pachyderma* left coiling). The ages were normalised for a $\delta^{13}\text{C}$ of 25‰ and corrected by -400 yr to account for the air-sea difference (for stratigraphical information see Hillaire-Marcel *et al.*, 1994, or the GEOTOP website). (c) Reconstruction of sea-surface parameters for core HU-84-030-021. Sea-surface temperature is in $^\circ\text{C}$. The dashed line corresponds to the best estimates using the $n = 371$ data base, and the solid line to the best estimates using the $n = 677$ data base with the modern analogue technique protocol as described in the text. The confidence interval calculated from the hydrographic values corresponding to the five best analogues in the $n = 677$ data base is shown by the grey zone. The distance of the best analogues is given on the right of the diagram (dashed line for the $n = 371$ data base, and solid line for the $n = 677$ data base). The arrows at the right margin of the best analogue distance curve point to a non-analogue situation using the $n = 371$ data base. Reconstructions for these two spectra are presented only using the $n = 677$ data base

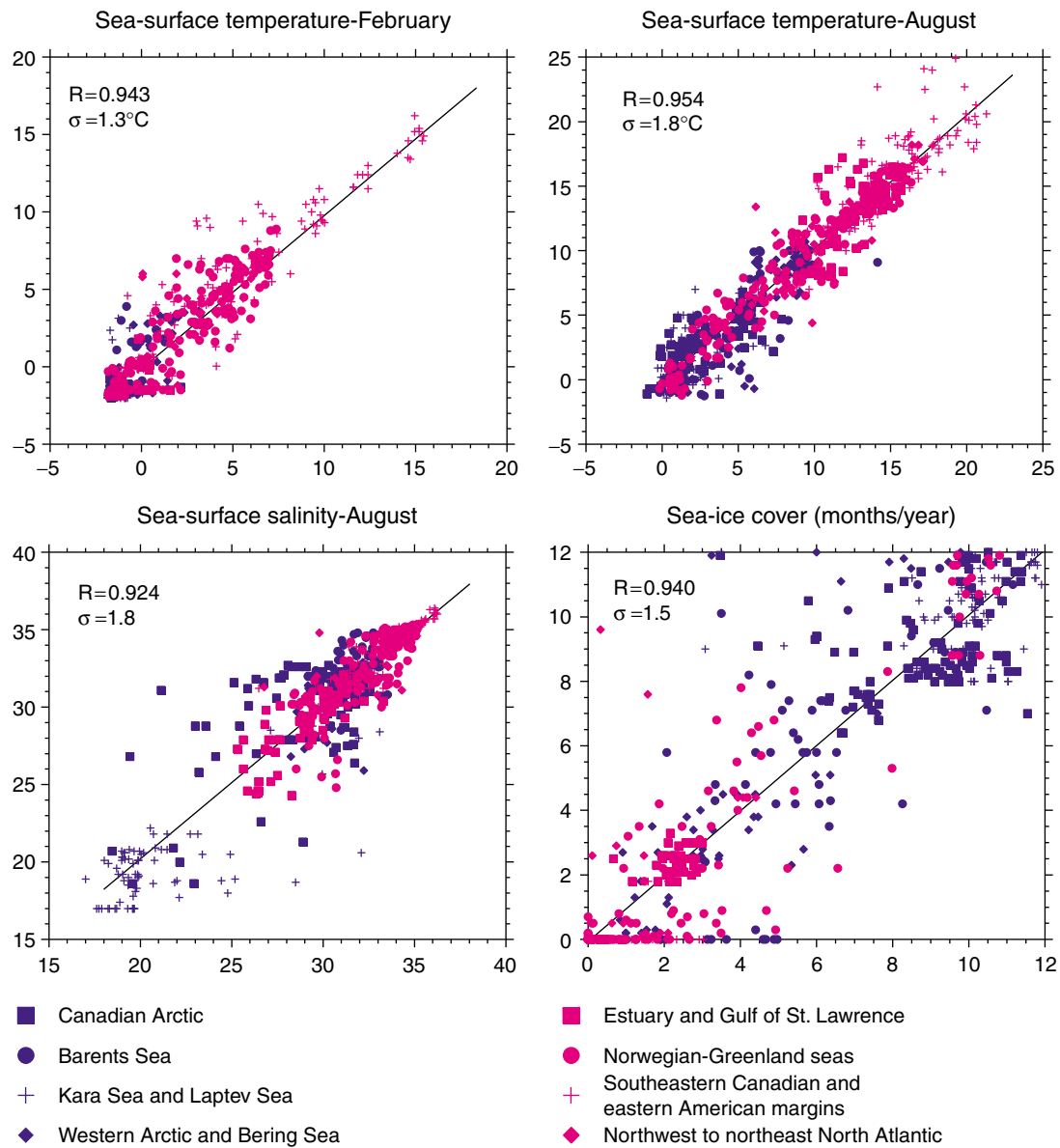


Plate 4 Results of the validation test for the reconstruction of sea-surface temperature, salinity and sea-ice cover after the procedure described in the text. The x -axis shows hydrographic averages resulting from instrumental observations, and the y -axis shows estimates from the dinocyst data. The coefficients of correlation (R) and the standard deviation σ of the difference between reconstruction and observation or root mean square error of prediction (RMSEP) provide the degree of accuracy of estimates (see text). These accuracy indicators were calculated for all data points ($n = 677$) although the prediction error clearly depends upon the geographical domain considered

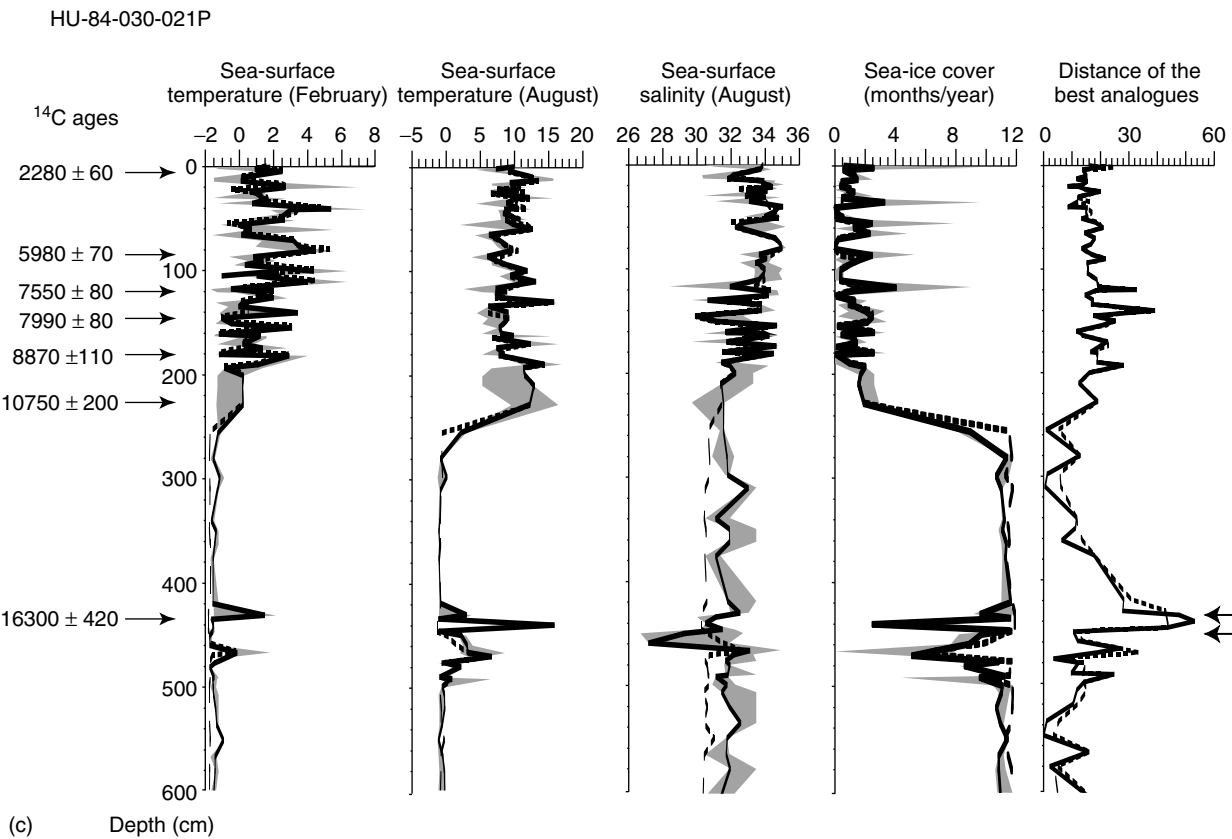
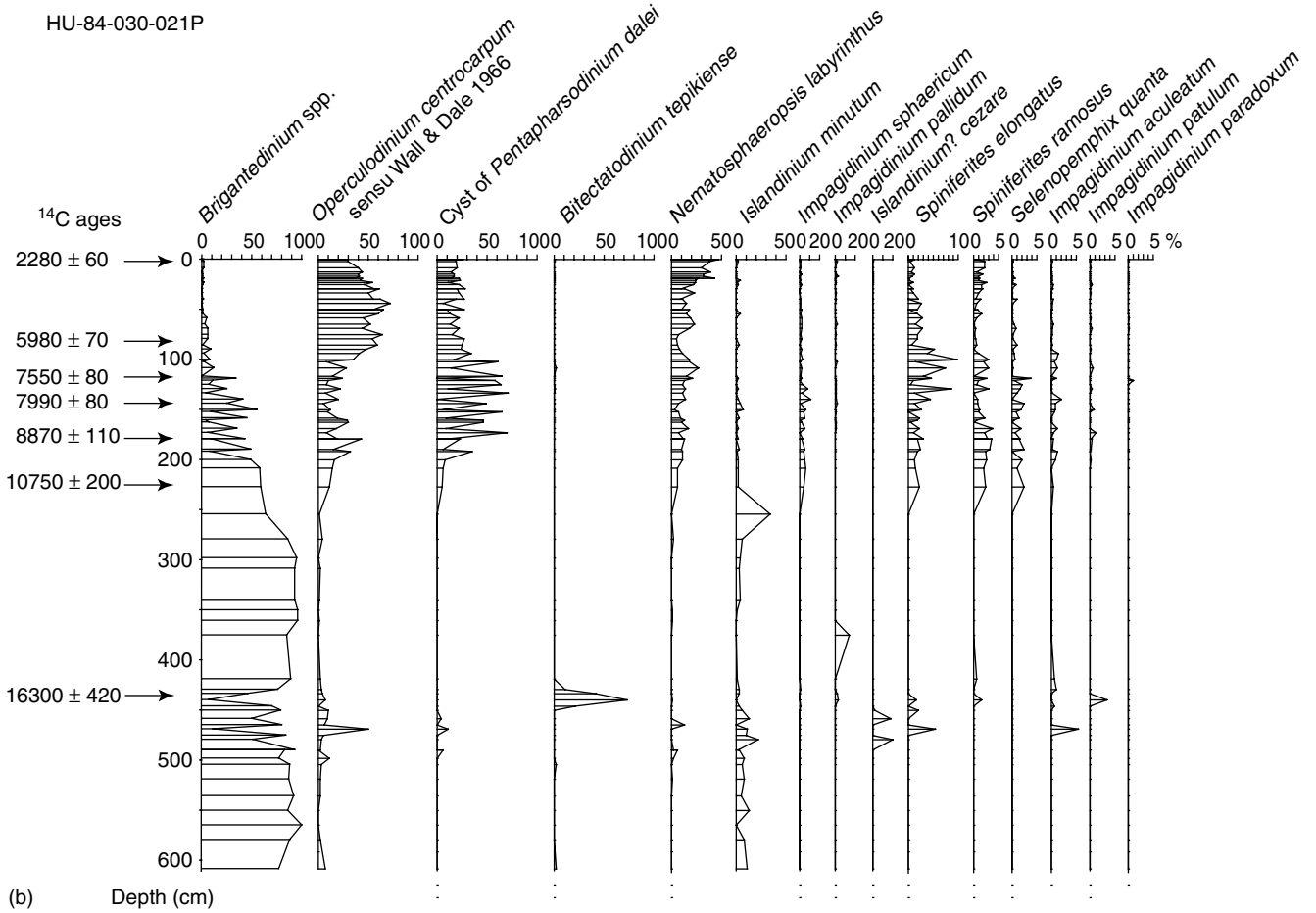


Figure 8 (Continued)

salinity averages 34.5 in August. Sea-ice cover develops only exceptionally (mean sea-ice = 0.5 month yr⁻¹). Modern dinocyst assemblages are characterised by the dominance of *Nematosphaeropsis labyrinthus* and *Operculodinium centrocarpum*, as are most other assemblages from offshore settings in the northwestern North Atlantic (cf. assemblage Va in Rochon *et al.*, 1999).

The stratigraphy of core HU-84-030-021 has been documented by de Vernal and Hillaire-Marcel (1987), and notably by Hillaire-Marcel *et al.* (1994) (see also the GEOTOP website). The stratigraphy shows a clear change in both lithology and palynological assemblages at the glacial–interglacial transition, which is dated around 11 000 ¹⁴C yr BP (Fig. 8b and c). This transition is marked by a change from glaciomarine sedimentation with abundant ice-rafting debris under cold conditions, to epipelagic sedimentation under oceanic and subpolar conditions. A major change in dinocyst assemblages also is recorded at this time. The glacial interval dated prior to ca. 11 000 ¹⁴C yr BP generally is characterised by assemblages dominated by *Brigantedinium* spp. and accompanied by *Islandinium minutum*. Above the transition, the assemblages are characterised by higher species diversity and the replacement of *Brigantedinium* spp. by *Operculodinium centrocarpum*, the cyst of *Pentapharsodinium dalei* and *Nematosphaeropsis labyrinthus*, which dominate the Holocene assemblages (Fig. 8b). The reconstruction of sea-surface conditions using both data sets reflects a major change at the glacial–interglacial transition, with a sharp decrease in sea-ice cover extent together with increasing temperature and salinity (cf. Fig. 8c).

In the post-glacial part of the record, the best analogues are found regionally and the distances are approximately identical whichever data base is used. The estimates are the same for all parameters considered and both curves of reconstruction are superimposed (Fig. 8c). In this case, it is clear that the *n* = 371 data base provided suitable analogues for reliable reconstructions. The use of the *n* = 677 data base also allows reliable reconstructions. In the lower part of the record, corresponding to the glacial episode, there are slight discrepancies between estimates depending upon the data base used. In general, the distance of analogues is slightly larger with the *n* = 371 data base. Closest analogues are found in the *n* = 677 data base, notably in the area of the North Water polynya, northernmost Baffin Bay, and in the Laptev Sea and northern Barents Sea, which were not represented in the *n* = 371 data base. Nevertheless, reconstructions of temperature and extent of sea-ice cover are almost identical whether using the *n* = 677 or *n* = 371 data base. The main discrepancy occurs in the reconstruction of salinity, which yields slightly higher values and has more fluctuations with the *n* = 677 data base. The *n* = 677 data base thus seems to be more sensitive to salinity than the *n* = 371 data base. Nevertheless, the reconstructions are consistent in as much as they both indicate low salinity (<32) during the glacial interval. Another point of interest in the record of the glacial interval is the peak of gonyaulacalean cysts, including *Bitectatodinium tepikiense*, that is recorded between 430 and 446 cm. The assemblages in this interval have poor analogues in both data bases, but particularly in the *n* = 371 data base, as the distance for the closest analogue is above the threshold value for two samples.

The Barents Sea

Core PL-96-112P (71°44.18N, 42°36.31E; 286 m), spanning the past 8500 yr (Voronina *et al.*, this issue), was collected on

the east Barents Shelf. This area is particularly interesting from a palaeoceanographical point of view because it presently constitutes the northernmost end-member of the North Atlantic Drift, at the boundary with Arctic waters flowing southward (see Fig. 9a; e.g. Loeng, 1991). At the coring site, sea-surface temperature is 7.8 ± 1.9 °C and 1.8 °C (σ unknown) in August and February respectively, with salinity in August of 34.8 ± 0.2. Sea-ice cover develops occasionally during the coldest years (mean sea-ice duration = 0.3 month yr⁻¹).

The dinocyst assemblages from core PL-96-112 have a high species diversity and generally are dominated by *Operculodinium centrocarpum*, the cyst of *Pentapharsodinium dalei*, and *Spiniferites elongatus*, these being accompanied notably by *Nematosphaeropsis labyrinthus* and *Brigantedinium* spp. (Fig. 9b). Throughout the sequence, the percentages of the main taxa record some tenuous variations. The most distinct trend, towards the top of the core, is the increased percentages of *Pentapharsodinium dalei* relative to a decrease in the occurrence of *Operculodinium centrocarpum*. Other variations in the assemblages that may be significant include fluctuations in the percentages of *Spiniferites elongatus*, maximum occurrence of *Nematosphaeropsis labyrinthus* between ca. 1500 and 3000 ¹⁴C yr BP, and sporadic occurrences of the cold water taxa *Islandinium minutum* and *Impagidinium pallidum*.

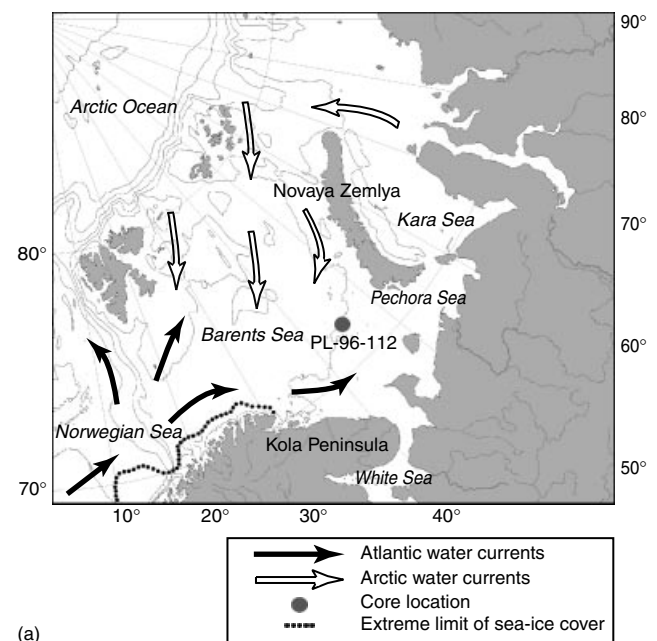


Figure 9 Location map and time series for Core PL96-112P, Barents Sea (71°44.18N–42°36.31E; 286 m) spanning the past 8500 yr. (a) Core location map showing the surface water circulation pattern. (b) Summary diagram of dinocyst assemblages. The chronological marks indicated in the left margins of the diagrams correspond to accelerator mass spectrometry (AMS) ¹⁴C ages on biogenic carbonates, which were normalised for a $\delta^{13}\text{C}$ of 25‰ and corrected by –460 yr to account for the regional air-sea difference (Voronina *et al.*, this issue). (c) Reconstruction of the sea-surface parameters. Sea-surface temperature is in °C. The dashed line corresponds to the best estimates using the *n* = 371 data base, and the solid line to the best estimates using the *n* = 677 data base with the modern analogue technique protocol as described in the text. The confidence interval calculated from the hydrographic values corresponding to the five best analogues of the *n* = 677 data base is shown by the grey zone. The distance of the best analogues is given on the right of the diagram (dashed line for the *n* = 371 data base, and solid line for the *n* = 677 data base)

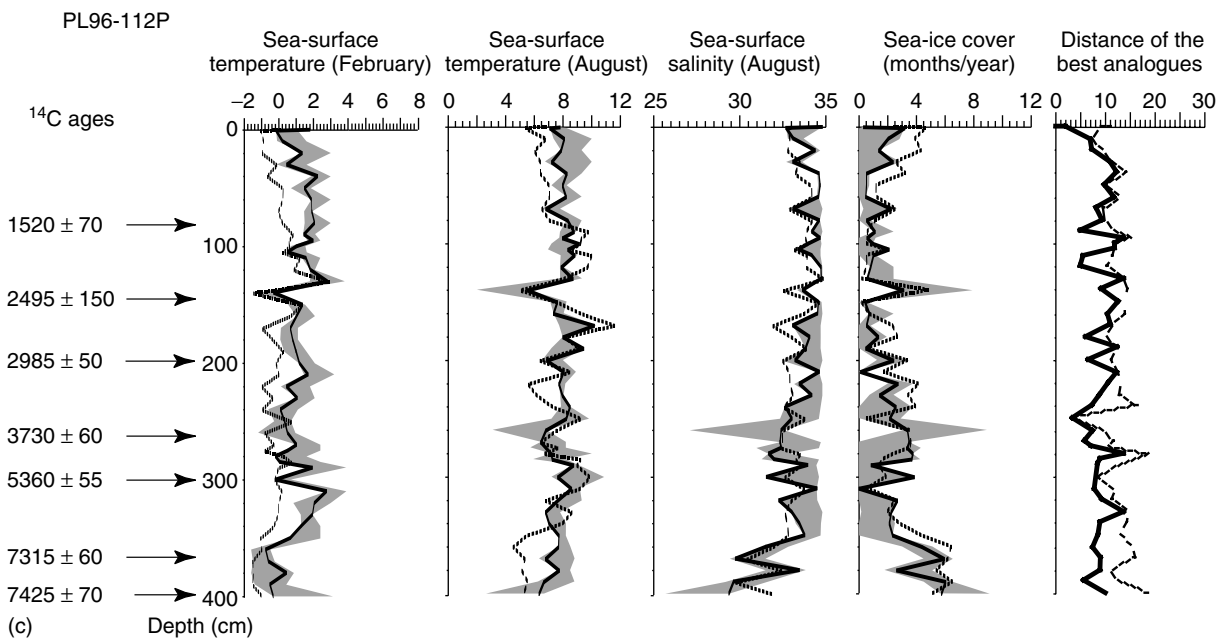
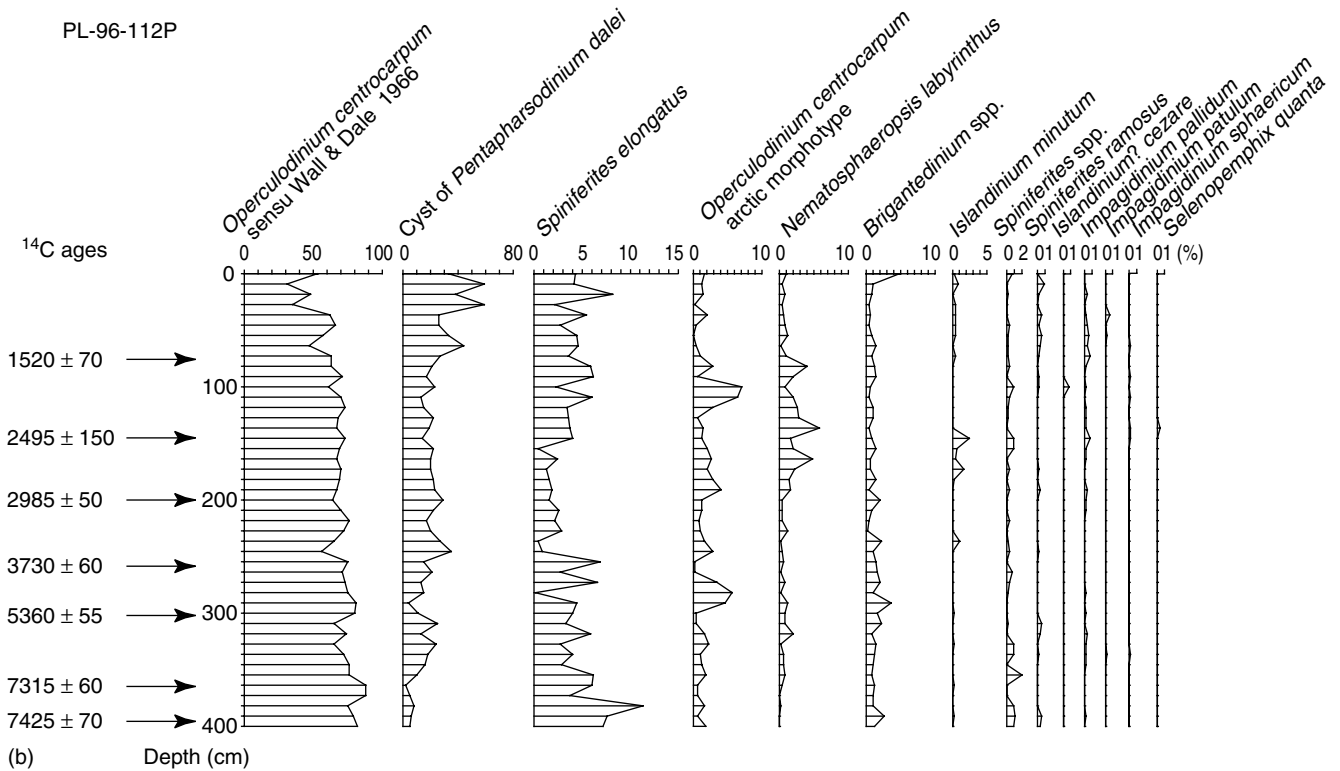


Figure 9 (Continued)

The reconstruction of sea-surface conditions in core PL-96-112 relies on different sets of analogues depending upon the data base considered (Fig. 9c). Both $n = 371$ and $n = 677$ data bases yield close analogues, with distances much lower than the threshold value, thus allowing estimations of hydrographic parameters. However, the distance is slightly larger when using the $n = 371$, the closest analogues being selected from the few available sites in the Barents Sea, in addition to sites from the Norwegian Sea and the Hudson Bay. When using the $n = 677$ data base, closer analogues are found in the Barents Sea and the eastern Arctic, in addition to sites from the Bering Sea, whereas spectra from the Norwegian Sea are selected only exceptionally. In spite of the different

selection of analogue spectra depending upon the data base used, the estimates of sea-surface conditions appear consistent. The variations in sea-ice cover and sea-surface salinity are almost superimposed, and the trend of increasing salinity recorded during the early–middle Holocene appears significant. There are slight discrepancies concerning the estimated temperatures. However, these discrepancies are not very important because they fall within the range of variations presently recorded at the coring site (i.e. $\pm 1.9^\circ\text{C}$ in August). Nevertheless, both reconstructions suggest limited changes in temperature, with the exception of a few cooling pulses, possibly significant, around 2500 and 3500–4000 ^{14}C yr BP, and prior to 8000 ^{14}C yr BP.

Discussion and conclusions

Uncertainties and limitations

The development of any technique for the reconstruction of past climatic parameters implies a number of approximations and assumptions. The main one is that the recent assemblages recovered in surface sediment samples are contemporaneous with the reference hydrographic data, which are averaged over a few tens of years. Another assumption is that the microfossil assemblages result from vertical fluxes from surface waters to the sea floor, and thus are representative of local sea-surface conditions above the coring site, with limited impact of lateral transport through intermediate or deep currents. Although the mechanisms of biogenic particle fluxes through the water column could be better documented, marine snow and fecal pellets in the area of plankton production no doubt contribute to rapid settling of micro-organism remains, which thus form microfossil assemblages with distribution patterns closely related with sea-surface conditions on a regional scale. The technique we have developed using dinocyst assemblages of the northern North Atlantic Ocean and circum-Arctic seas bears a few additional particularities.

- 1 Several new morphotypes are apparently characteristic of Arctic seas. Although it is uncertain whether they are ecophenotypic variants or new taxa, their ecological and biological affinities still need documenting.
- 2 The rarity of hydrographic measurements in the Arctic domain, and the lack of consistent oceanographic data on a hemispheric scale constitute a real problem. We hope such data will be available in the near future, and will contribute to the improvement of the accuracy of the proposed technique of reconstruction.
- 3 In Arctic environments that are marked by large freshwater discharges such as the Laptev Sea (e.g. Kunz-Pirrung, this issue), the upper water masses may be characterised by a very shallow halocline or pycnocline (<20 m). Although we are using the surface layer (0 m) to establish relationships with dinocyst assemblages, we cannot demonstrate that original dinoflagellate populations are indeed living above the pycnocline in such nearshore environments. This could be a source of error, which could partly explain the limited accuracy of salinity reconstructions in the low-salinity domain. We have tried to raise a data base of hydrographic conditions within the water column in order to address this question. However, here again the scarcity of data prevents any reasonable statistical treatment.
- 4 It is unquestionable on empirical grounds that dinocyst assemblages are related to the distribution of temperature, salinity and sea-ice cover in surface waters. However, the dinocyst assemblages also are dependent upon other parameters as shown by principal component analyses. These parameters may be linked to nutrient distribution or to the trophic structure of planktonic populations (e.g. Devillers and de Vernal, 2000). For example, in Arctic environments, the distribution of dinocyst assemblages, and particularly the proportion of Gonyaulacales versus Peridinales show close relationships with the distribution of polynyas (e.g. Hamel, 2001).

The choice of a conservative approach

Despite the above-mentioned uncertainties or limitations it has been possible to develop a reasonably accurate technique for the reconstruction of sea-surface conditions based on the artificial neural network technique (Peyron and de Vernal, this issue) and on the basis of the best-analogue method, as presented here. The approach described in the present paper is rather conservative. It relies on interpolation and so cannot yield reconstructions outside the range of modern hydrographic conditions. Moreover, by using threshold values to identify non-analogue situations, we avoid speculative reconstruction when assemblages reveal different situations to those represented by the modern environment. Of course, such an approach requires a large reference data base. As the $n = 371$ and $n = 677$ data bases yield consistent results for subarctic seas adjacent to the northwest and northeast North Atlantic, we may assume that they are both adequate for reconstructions in the subpolar domain. Moreover, the $n = 677$ covers a geographical and hydrographic domain wide enough to permit reconstruction of past sea-surface conditions in circum-Arctic regions.

Acknowledgements This work is a contribution to the Canadian research project 'Climate System History and Dynamics' (CSDH), funded by the Natural Science and Engineering Research Council (NSERC) of Canada. Additional support was provided to ADV by the *Fonds pour la Formation de Chercheurs et l'aide à la Recherche* (FCAR) of Quebec. The *Institut Français pour la Recherche et la Technologie Polaires* (IFRTP) provided logistical support to JLT and FE, who also thank the French CNRS, the *Programme National d'Etude du Climat* (PNEDC), and the European Community for financial support. JM and MKP thank the German Science Foundation (DFG) and the German Ministry for Education, Science, Research and Technology (BMBF). MJH is grateful to Wolfson College, Cambridge for a Visiting Fellowship. The work of VP was supported by NSERC-Canada. The data base presented here has been developed through access to sediment samples or data provided by many Canadian, American and European Institutions. We wish to thank particularly Oregon State University, the Geological Survey of Canada, and the Byrd Polar Research Center for access to surface sediment samples. We are grateful to the reviewers, Fabienne Marret and Michal Kucera, for their critical comments, which were most helpful to prepare the revised version of the manuscript.

References

- Birks HJB. 1995. Quantitative palaeoenvironmental reconstructions. In *Statistical Modelling of Quaternary Science Data*, Maddy D, Brew JS (eds). Technical Guide, Quaternary Research Association: Cambridge; 161–254.
- Boessenkool KP, van Gelder M-J, Brinkhuis H, Troelstra SR. 2001. Distribution of organic-walled dinoflagellate cysts in surface sediments from transects across the Polar Front offshore southeast Greenland. *Journal of Quaternary Science* **16**: 661–666.
- Dale B. 1983. Dinoflagellate resting cysts: 'benthic plankton'. In *Survival strategies of the algae*, Fryxell GA (ed). Cambridge University Press: Cambridge; 69–137.
- Dale B. 1996. Dinoflagellate cyst ecology: modeling and geological applications. In *Palynology: Principles and Applications*. Jansounius J, McGregor DC (eds). American Association of Stratigraphic Palynologists: Dallas, TX; 1249–1275.
- Deflandre G, Cookson IC. 1955. Fossil microplankton from Australian Late Mesozoic and Tertiary sediments. *Australian Journal of Marine and Freshwater Research* **6**: 242–313.
- De Vernal A, Hillaire-Marcel C. 1987. Marginal paleoenvironments of the eastern Laurentide ice sheet and timing of the last ice maximum and retreat. *Géographie physique et Quaternaire* **XLI**: 265–277.

- De Vernal A, Hillaire-Marcel C. 2000. Sea-ice cover, sea-surface salinity and halothermocline structure of the northwest North Atlantic: modern versus full glacial conditions. *Quaternary Science Reviews* **19**: 65–85.
- De Vernal A, Goyette C, Rodrigues C. 1989. Contribution palynostratigraphique (dinokystes, pollen et spores) à la connaissance de la mer de Champlain: coupe de Saint-Cézaire, Québec. *Canadian Journal of Earth Sciences* **26**: 2450–2464.
- De Vernal A, Rochon A, Hillaire-Marcel C, Turon J-L, Guiot J. 1993a. Quantitative reconstruction of sea-surface conditions, seasonal extent of sea-ice cover and meltwater discharges in high latitude marine environments from dinoflagellate cyst assemblages. In *Proceedings of the NATO Workshop on Ice in the Climate System*, Springer-Verlag: Berlin, NATO ASI Series Vol. **112**: 611–621.
- De Vernal A, Guiot J, Turon J-L. 1993b. Postglacial evolution of environments in the Gulf of St. Lawrence: palynological evidence. *Géographie physique et Quaternaire* **47**: 167–180.
- De Vernal A, Turon J-L, Guiot J. 1994. Dinoflagellate cyst distribution in high-latitude marine environments and quantitative reconstruction of sea-surface salinity, temperature, and seasonality. *Canadian Journal of Earth Sciences* **31**: 48–62.
- De Vernal A, Hillaire-Marcel C, Bilodeau G. 1996. Reduced meltwater outflow from the Laurentide ice margin during the Younger Dryas. *Nature* **381**: 774–777.
- De Vernal A, Rochon A, Turon J-L, Matthiessen J. 1997. Organic-walled dinoflagellate cysts: palynological tracers of sea-surface conditions in middle to high latitude marine environments. *Géobios* **30**: 905–920.
- De Vernal A, Henry M, Bilodeau G. 1999. *Technique de préparation et d'analyse en micropaléontologie*. Unpublished Report 3, Les Cahiers du GEOTOP, Université du Québec à Montréal.
- De Vernal A, Hillaire-Marcel C, Turon J-L, Matthiessen J. 2000. Reconstruction of sea-surface temperature, salinity, and sea-ice cover in the northern North Atlantic during the last glacial maximum based on dinocyst assemblages. *Canadian Journal of Earth Sciences* **37**(5): 725–750.
- Devillers R, de Vernal A. 2000. Distribution of dinocysts in surface sediments of the northern North Atlantic in relation with nutrients and productivity in surface waters. *Marine Geology* **166**: 103–124.
- Eynaud F. 1999. *Kystes de Dinoflagellés et Evolution paléoclimatique et paléohydrologique de l'Atlantique Nord au cours du Dernier Cycle Climatique du Quaternaire*, Université de Bordeaux I; 291 pp.
- Grøsfjeld K, Harland R. Distribution of modern dinoflagellate cysts from inshore areas along the coast of southern Norway. *Journal of Quaternary Science* **16**: 651–659.
- Grøsfjeld K, Larsen E, Sejrup HP, de Vernal A, Flatebø T, Vestbø M, Hafliðason H, Aarseth I. 1999. Dinoflagellate cysts reflecting surface-water conditions in Voldafjorden, western Norway during the last 11 300 years. *Boreas* **28**: 403–415.
- Guiot J. 1990. Methodology of paleoclimatic reconstruction from pollen in France. *Palaeogeography, Palaeoclimatology, Palaeoecology* **80**: 49–69.
- Guiot J, Goeury C. 1996. PPPbase, a software for statistical analysis of paleoecological data. *Dendrochronologia* **14**: 295–300.
- Hamel D. 2001. *Les palynomorphes et traceurs géochimiques: marqueurs de la productivité des cinq derniers siècles dans les eaux du Nord et le Nord de la Baie de Baffin (75–79° N, 66–80° W)*, Mémoire de Maîtrise, Université du Québec à Rimouski.
- Harland R. 1981. Cysts of the colonial dinoflagellate *Polykrikos schwartzii* Bütschli 1873, (Gymnodinales), from Recent sediments, Firth of Forth, Scotland. *Palynology* **5**: 65–79.
- Harland R. 1983. Distribution maps of Recent dinoflagellate cysts in bottom sediments from the North Atlantic Ocean and adjacent seas. *Palaeontology* **26**: 321–387.
- Harland R, Pudsey CJ. 1999. Dinoflagellate cysts from sediment traps deployed in the Bellingshausen, Weddell and Scotia seas, Antarctica. *Marine Micropaleontology* **37**: 77–99.
- Head MJ. 1996a. Modern dinoflagellate cysts and their biological affinities. In *Palynology: Principles and Applications*, Jansonius J, McGregor DC (eds). American Association of Stratigraphic Palynologists Foundation: Dallas, TX; Vol. 3: 1197–1248.
- Head MJ. 1996b. Paleoeological and taxonomic revision of late Cenozoic dinoflagellates from the Royal Society borehole at Ludham, eastern England. *Journal of Paleontology* **70**: 543–570.
- Head MJ, Harland R, Matthiessen J. Cold marine indicators of the late Quaternary: the new dinoflagellate cyst genus *Islandinium* and related morphotypes. *Journal of Quaternary Science* **16**: 621–636.
- Hillaire-Marcel C, de Vernal A, Bilodeau G, Wu G. 1994. Isotope stratigraphy, sedimentation rates and palaeoceanographic changes in the Labrador Sea. *Canadian Journal of Earth Sciences* **31**: 63–89.
- Hillaire-Marcel C, de Vernal A, Bilodeau G, Weaver AJ. 2001a. Absence of deep water formation in the Labrador Sea during the last interglacial period. *Nature* **410**: 1073–1077.
- Hillaire-Marcel C, de Vernal A, Candon L, Bilodeau G, Stoner J. 2001b. Changes of potential density gradients in the northwestern North Atlantic during the last climatic cycle based on a multiproxy approach. In *Instabilities in the climate system*, Seidov D, et al. (eds). Geophysical Monograph Series: Washington, DC, **126**: 83–100.
- Hutson WH. 1980. The Agulhas current during the late Pleistocene: Analysis of modern faunal analogs. *Science* **207**: 64–66.
- Imbrie J, Kipp NG. 1971. A new micropaleontological method for quantitative paleoclimatology: application to a late Pleistocene Caribbean core. In *The Late Cenozoic Glacial Ages*, Turekian KK (ed.). Yale University Press: New Haven, CN, 71–179.
- Kucera M, Malmgren BA. 1998. Logratio transformation of compositional data—a resolution of the constant sum constraint. *Marine Micropaleontology* **34**: 117–120.
- Kunz-Pirrung M. 1998. Rekonstruktion der Oberflächenwassermassen der östlichen Laptevsee im Holozän anhand von aquatischen Palynomorphen. *Berichte zur Polarforschung* **281**: 117.
- Kunz-Pirrung M. 2001. Dinoflagellate cyst assemblages in surface sediments of the Laptev Sea region (Arctic Ocean) and their relationship to hydrographic conditions. *Journal of Quaternary Science* **16**: 637–649.
- Levac E, de Vernal A. 1997. Postglacial changes of terrestrial and marine environments along the Labrador coast: palynological evidence from cores 91-045-005 and 91-045-006, Cartwright Saddle. *Canadian Journal of Earth Sciences* **34**(10): 1358–1365.
- Levac E, de Vernal A, Blake Jr W. 2001. Sea-surface conditions in northernmost Baffin Bay during the Holocene: palynological evidence. *Journal of Quaternary Science* **16**: 353–363.
- Loeng H. 1991. Features of the physical oceanographic conditions of the Barents Sea. *Polar Research* **10**: 5–18.
- Malmgren B, Nordlund U. 1997. Application of artificial neural network to palaeoceanographic data. *Palaeogeography, Palaeoclimatology, Palaeoecology* **136**: 359–373.
- Malmgren B, Kucera M, Nyberg J, Waelbroeck C. 2001. Comparison of statistical and artificial neural network techniques for estimating past sea-surface temperatures from planktonic foraminifer census data. *Paleoceanography* **16**: in press.
- Markham WE. 1980. *Atlas des glaces, littoral de l'est canadien*. Environnement Canada, Atmospheric Environment Service: Ottawa, Ontario.
- Marret F. 1993. Les effets de l'acétolyse sur les assemblages de kystes de dinoflagellés. *Palynosciences* **2**: 267–272.
- Matthiessen J. 1995. Distribution patterns of dinoflagellate cysts and other organic-walled microfossils in recent Norwegian–Greenland Sea sediments. *Marine Micropaleontology* **24**: 307–334.
- McCarthy FM, Gostlin KE, Mudie PJ, Scott DB. 2000. Synchronous palynological changes in Early Pleistocene sediments off New Jersey and Iberia, and a possible palaeoceanographic explanation. *Palynology* **24**: 63–77.
- Mudie PJ. 1992. Circum-Arctic Quaternary and Neogene marine palynofloras: paleoecology and statistical analysis. In *Neogene and Quaternary Dinoflagellate Cysts and Acritarchs*, Head MJ, Wrenn JH (eds). American Association of Stratigraphic Palynologists Foundation: Dallas, TX: 347–390.
- Mudie PJ, Rochon A. 2001. Distribution of dinoflagellate cysts in the Canadian Arctic marine region. *Journal of Quaternary Sciences* **16**: 603–620.
- Mudie PJ, Short SK. 1985. Marine palynology of Baffin Bay. In *Quaternary Environments*, Andrews JT (ed.). Allen & Unwin: Boston, London, Sydney; 263–308.
- NODC. 1994. *World Ocean Atlas*. National Oceanographic Data Center, National Oceanic and Atmospheric Administration: Boulder, CO, CD-Rom data Sets.
- Peyron O, de Vernal A. 2001. Application of artificial neural networks (ANN) to high-latitude dinocyst assemblages for the reconstruction

- of past sea-surface conditions in Arctic and sub-Arctic seas. *Journal of Quaternary Science* **16**: 699–709.
- Peyron O, Guiot J, Cheddadi R, Tarasov PE, Reille M, de Beaulieu J-L, Bottema S, Andrieu V. 1998. Climatic reconstruction in Europe for 18,000 yr B.P. from pollen data. *Quaternary Research* **49**: 183–196.
- Peyron O, Jolly D, Bonnefille R, Vincens A, Guiot J. 2000. Climate of East Africa 6000 ¹⁴C yr B.P. as inferred from pollen data. *Quaternary Research* **54**: 90–101.
- Pflaumann U, Duprat J, Pujol C, Labeyrie L. 1996. SIMMAX: a modern analog technique to deduce Atlantic sea surface temperatures from planktonic foraminifera in deep-sea sediments. *Paleoceanography* **11**: 15–35.
- Prell W. 1985. *The Stability of Low-Latitude Sea-surface Temperatures: an Evaluation of the CLIMAP Reconstructions with Emphasis on the Positive SST Anomalies*. Technical Report TR025, US Department of Energy: Washington, DC; 60 pp.
- Radi T, de Vernal A, Peyron O. 2001. Relationships between dinoflagellate cyst assemblages in surface sediment and hydrographic conditions in the Bering and Chukchi seas. *Journal of Quaternary Science* **16**: 667–680.
- Rochon A, de Vernal A. 1994. Palynomorph distribution in recent sediments from the Labrador Sea. *Canadian Journal of Earth Sciences* **31**: 115–127.
- Rochon A, de Vernal A, Sejrup HP, Hafliðason H. 1998. Climatic change and sea-surface conditions during the deglaciation: palynological evidences from the North Sea. *Quaternary Research* **49**: 197–207.
- Rochon A, de Vernal A, Turon J-L, Matthiessen J, Head MJ. 1999. *Distribution of Dinoflagellate Cyst Assemblages in Surface Sediments from the North Atlantic Ocean and Adjacent Basins and Quantitative Reconstruction of Sea-surface Parameters*. Special Contribution Series 35, American Association of Stratigraphic Palynologists: Dallas, TX.
- Taylor FJR (ed.). 1987. *The Biology of Dinoflagellates*. Botanical Monographs (Oxford), Vol. 21, Blackwell Scientific publications: Oxford; 785 pp.
- Ter Braak CJF, van Dam H. 1989. Inferring pH from diatoms: a comparison of old and new calibration methods. *Hydrobiologia* **178**: 209–223.
- Turon J-L. 1984. *Le palynoplancton dans l'environnement actuel de l'Atlantique nord-oriental. Évolution climatique et hydrologique depuis le dernier maximum glaciaire*. Doctorat ès sciences thesis, Université Bordeaux I, *Mémoire de l'Institut de Géologie du Bassin d'Aquitaine* **17**: 313 p.
- Voronina E, Polyak L, de Vernal A, Peyron O. 2001. Holocene variations of sea-surface conditions in the southeastern Barents Sea, reconstructed from dinoflagellate cyst assemblages. *Journal of Quaternary Science*, **16**: 717–726.
- Waelbroeck C, Labeyrie L, Duplessy J-C, Guiot J, Labracherie M, Leclaire H, Duprat J. 1998. Improving paleo-SST estimates based on planktonic fossil faunas. *Paleoceanography* **12**: 272–283.
- Wall D, Dale B. 1966. 'Living fossils' in western Atlantic plankton. *Nature* **211**: 1025–1026.
- Zonneveld KA, Versteegh GH, de Lange GJ. 2001. Paleoproductivity and postdepositional aerobic organic matter decay reflected by dinoflagellate cyst assemblages in Eastern Mediterranean S1 Sapropoel. *Marine Geology*, **172**: 181–195.